TECHNICAL NOTES

NATIONAL ADVISORY COMMITTEE FOR AERONAUTICS

No. 791

SHEAR LAG IN CORRUGATED SHEETS USED FOR THE CHORD MEMBER OF A BOX BEAM

By Joseph S. Newell and Eric Reissner
Massachusetts Institute of Technology

Washington
January 1941

NATIONAL ADVISORY COMMITTEE FOR AERONAUTICS

TECHNICAL NOTE NO. 791

SHEAR LAG IN CORRUGATED SHEETS USED FOR THE CHORD MEMBER OF A BOX BEAM

By Joseph S. Newell and Eric Reissner

SUMMARY

The problem of the distribution of normal stress across a wide corrugated sheet used as the chord of a box-beamlike structure is investigated theoretically and experimentally. Expressions are developed giving the stress distribution in beams symmetrical or unsymmetrical about a plane passed spanwise through the center of the sheet. The experiments were arranged to insure bending without torsion and surveys of the normal stresses were made by means of mechanical and electrical strain gages.

The experimental data showed very good agreement with the shape of the theoretical curves, especially at the highly stressed sections, for both the symmetrical and unsymmetrical beams.

Several suggestions for future research are included.

INTRODUCTION

This paper is presented in two parts. In part I, expressions are developed for the distribution of normal stress across a wide corrugated sheet used as the chord of a box beam, regard being given to the variation in normal stress resulting from shear lag in the sheet. The developed expressions cover the cases of symmetrical and unsymmetrical box beams with respect to a plane passed spanwise through the center of the sheet.

In part II of the paper, the experimental results are presented. Strain-gage surveys were made to obtain the distribution of normal stresses across a series of sections of the corrugated sheet. Huggenberger tensometers were used for the symmetrical beam, and both Huggenberger tensometers and a fine-wire electrical gage were used for the unsymmetrical specimen. Because the corrugated sheet was not perfectly flat and because complications due to possible increased buckling of the sheet were to be avoided, the beams were always loaded so that the sheet formed the tension chord of the box.

Inasmuch as more data were obtained for the unsymmetrical specimen, the data for that beam are somewhat more definite than for the symmetrical. The shape of the stress-distribution curves at all sections is in general accord with the developed theory.

The theoretical procedure presented in part I is the work of Dr. Eric Reissner of the Department of Mathematics of the Massachusetts Institute of Technology. At his suggestion, Hymen Katz investigated the effect of varying certain transverse stiffnesses on the symmetrical beam; the data credited to him are taken from reference 1.

Aldridge (reference 2) and Amarante (references 3 and 4) carried out the experimental work on the symmetrical beam. The test data are taken from references 2, 3, and 4; most of the work was from the tests of Amarante, who investigated several cross sections of the beam.

The wire-resistance strain gages were developed by Prof. A. C. Ruge of Massachusetts Institute of Technology. They were adapted for use on the corrugated sheet by W. T. Shuler, who also made the stress surveys on the unsymmetrical beam.

The entire project was carried out under the supervision of Prof. J. S. Newell of the Aeronautics Department of the Massachusetts Institute of Technology. It was made possible by financial assistance from the National Advisory Committee for Aeronautics under its program for fostering research in educational institutions.

PART I - THEORETICAL INVESTIGATION

A - SCOPE OF THE THEORY DEVELOPED

The present theory of the shear lag may be considered as occupying a position intermediate between those proposed by Von Kármán, Reissner, Younger, Kuhn, and Ebner and Köller. (See references 5 to 8, and 10.) It was first presented in 1938 (reference 9) without, however, elucidating its relation to the existing theories. It may be briefly described by saying that it is applicable to the problems of Von Kármán and Younger without being of the same mathematical complexity and that it may be used on problems to which Kuhn's, and Ebner and Köller's theories are not applicable.

The relation between the different theories will be brought out in section B. In section C, the present theory is applied to the analysis of a symmetrical one-bay beam; calculations previously reported in references 1 and 9 have been partly repeated and extended. In section D the theory is used for the analysis of an unsymmetrical one-bay beam under unsymmetrical loading conditions. The procedure used with this case has not been published previously.

B - THE MATHEMATICAL FUNDAMENTALS OF THE SHEAR-LAG THEORY

DESCRIPTION OF THE STRUCTURE ANALYZED

The fundamentals of the shear-lag theory are best explained by considering one simple structure; a symmetrical box beam characterized by the following data is utilized here (see fig. 1):

The span length l.

The width $2w$. With corrugated sheet, $2w$ is the developed width of the corrugated sheet, being c times the projected width where c is a coefficient depending upon the pitch-depth ratio of the corrugation.

The moment of inertia of the side beam and cover plates, I_o.

The thickness of the cover sheet, t.

The elastic moduli of the cover sheet.

The cross-sectional area A of a stringer symmetrically attached to the cover sheet, if a stringer be used.

This box beam is assumed to be rigidly supported at one end and to be loaded at the free ends of the side beams.

The aim of the procedure developed here is the determination of the distribution of stress in the cover sheet, in the side beams, and in the middle stiffener if one be used. The need for such a procedure was shown by strain surveys on airplane wings, which demonstrated that all regions of the cover sheet would not be equally effective and, consequently, that the elementary beam theory which assumed uniform normal stress distribution across the cover sheet was no longer sufficiently accurate.

The cover sheets being flat and without load normal to their plane and the sheet thickness t small compared with the height h of the beam, it follows that the problem of the determination of the stresses in the sheet can be classified as a problem of plane stress.

THE FUNDAMENTALS OF THE THEORY OF PLANE STRESS

It is well known that the theory of plane stress leads to a set of differential equations involving three stress components and two displacement components and that these equations are made complete by the addition of a set of boundary conditions which express the manner in which the loads are introduced into the sheet.

In the following discussion it is essential that the sheet be considered an anisotropic material, that is, a material possessing elastic properties different in its transverse and longitudinal directions. One of the purposes of this section is, in fact, to point out that the various existing theories distinguish themselves only by making different assumptions concerning the anisotropy of the sheet material.

The fundamental plane-stress equations are:

a) The equations of equilibrium for the three stress components

$$\frac{\partial \sigma_x}{\partial x} + \frac{\partial \tau}{\partial y} = 0 \tag{1a}$$

$$\frac{\partial \tau}{\partial x} + \frac{\partial \sigma_y}{\partial y} = 0 \tag{1b}$$

b) The stress-strain relations involving the stress components and the displacement components u and v, which are, for an anisotropic material of the kind here considered,

$$E_x \frac{\partial u}{\partial x} = \sigma_x - \nu_x \sigma_y \tag{2a}$$

$$E_y \frac{\partial v}{\partial y} = \sigma_y - \nu_y \sigma_x \tag{2b}$$

$$G \left(\frac{\partial u}{\partial y} + \frac{\partial v}{\partial x}\right) = \tau \tag{2c}$$

In these equations, E_x denotes the modulus of elasticity in spanwise and E_y in transverse direction if a system of coordinates x,y be introduced where the x-direction is the spanwise and the y-direction the transverse. The symbol G denotes the shear modulus. (As long as the sheet is not wrinkled, G is a constant of the material. For sheets wrinkled under the influence of stress, it is customary to denote G as the reduced shear modulus, the amount of reduction depending on the extent to which wrinkles are developed. No consideration is, however, given to this aspect of the problem in the present investigation.) The constants ν_x and ν_y are two Poisson's ratios. For the existence of a strain-energy function, it is necessary that the following relation exist between the elastic constants:

$$\nu_y E_x = \nu_x E_y \tag{3}$$

Concerning the boundary conditions, it is necessary only to state at this place that they express the conditions of support as well as the condition that the strains in the side beams and stiffeners must coincide with those of the sheet along all junctions and that each element of these members must be in equilibrium under the influence of the external forces and of the edge shear of the sheet acting on the element.

A DISCUSSION OF THE EXISTING SOLUTIONS

The basic equations (1) and (2) being available, it is possible to state the differences between the existing solutions of the shear-lag problem as follows:

(a) Von Kármán (reference 5):

$$E_x = E_y = E, \quad \nu_x = \nu_y = \nu, \quad G = \frac{E}{2(1 + \nu)}$$

(b) Younger (reference 7):

$$E_x = E, \quad E_y = \infty, \quad \nu_x = \nu_y = 0$$

(c) Kuhn (reference 8):

$$E_x = 0, \quad E_y = \infty, \quad \nu_x = \nu_y = 0$$

(d) Reissner (reference 9):

$$E_x = E, \quad E_y = 0, \quad \nu_x = \nu, \quad \nu_y = 0, \quad G = \frac{E}{2(1 + \nu)}$$

(e) Ebner and Köller (reference 10):

$$E_x = 0, \quad E_y = 0, \quad \nu_x = \nu_y = 0$$

The foregoing conditions indicate that Von Kármán considered an isotropic sheet, Younger a sheet elastic in the spanwise direction but rigid in the transverse, Kuhn a sheet having no spanwise elasticity but rigid transversely. Reissner's solution presupposes a material elastic in the spanwise direction and not resistant transversely, while Ebner and Köller consider a sheet material entirely lacking in resistance to normal stresses and effective only in shear.

Solutions (a) and (b) have a certain disadvantage in that the mathematical difficulty in satisfying all boundary conditions may be great, it having been surmounted at present only for certain types of boundary conditions. The solvable cases may be characterized by the statement that for them the structure considered must be part of a beam infinitely extended in the spanwise direction and subjected to a periodic load distribution. For a beam of finite span - length equal to 1, 1/2, or 1/4 period - this requires that the following conditions are satisfied at the ends: Either shear stress and spanwise displacement are simultaneously zero, or normal stress and transverse displacement are simultaneously zero. Whereas the second condition describes the state of stress at the free end of a beam rather well, it is uncertain to what extent the first condition of vanishing shear along a built-in edge may reduce the accuracy of the solution in the neighborhood of the edge when applied to actual problems.

Kuhn's solution (c) may be said to be eminently applicable if the structure is such that the axial load carrying capacity of the sheets is insignificant compared with the corresponding capacity of the stringer material. If, however, most of the axial normal stress is carried by the sheets, as would occur with corrugated cover sheets, his theory does not appear to apply.

It was for this case that solution (d) was developed. This theory gives essentially the results of theories (a) and (b) without being of the same mathematical difficulty, the simplifying assumption involved being that the transverse normal stresses which accompany the shear and spanwise normal stress, but are not in themselves of primary interest, are not carried by the sheet itself but by transverse stiffeners. The specific advantage of this theory is that it is possible to satisfy any boundary condition which may occur along transverse sections. It is thought that this theory is applicable to flat sheets as well as corrugated, when the corrugated sheets are considered as nonisotropic flat sheets. Owing to the neglected transverse resistance of the material, it is to be expected that the results are closer to reality for corrugated than for flat sheets, which is one of the reasons for testing a beam with corrugated cover.

The theory of Ebner and Köller (reference 10) goes further. It neglects the resistance of the sheet to both transverse and spanwise normal stresses and takes into consideration only the normal-stress-carrying capacity of the stiffener and the shear-stress-carrying capacity of the sheet. Therefore, the remarks made about Kuhn's theory also apply here. One observation which should be added, however, is that the Ebner-Köller theory is essentially a framework theory and the methods developed for the treatment of statically indeterminate frameworks can therefore be applied to permit the analysis of rather complicated structures.

THE GENERAL SOLUTION FOR THE SHEET WITHOUT TRANSVERSE STIFFNESS

In this section the general solution, as previously derived in reference 9, of the equations (1) and (2) is given for the case (d):

$$E_x = E, \quad E_y = 0$$

It is written in the form

$$\sigma_y = 0 \tag{3a}$$

$$\tau = f(y) \tag{3b}$$

$$\sigma_x = -xf'(y) + g(y) \tag{3c}$$

$$E\,u = -\frac{1}{2}x^2 f'(y) + xg(y) + h(y) \tag{4a}$$

$$E\,v = \frac{1}{6}x^3 f''(y) - \frac{1}{2}x^2 g'(y) - xh'(y) + \left(\frac{E}{G}\right)xf(y) + k(y) \tag{4b}$$

where f, g, h, and k are four arbitrary functions. The solution is to be obtained by direct integration of equations (1) and (2); the arbitrary functions in the solution are determined from conditions along transverse sections of the beam, and the remaining arbitrary constants are determined from conditions along the junction between side webs and sheets, or stringers and sheets.

C - SHEAR LAG IN A SYMMETRICAL BEAM UNDER SYMMETRICAL LOADING CONDITIONS

THE BEAM WITH AXIALLY RIGID TRANSVERSE END STIFFENER

In this section the stress distribution in the cover sheet of the beam that was investigated experimentally is determined theoretically. A beam is considered carrying a cover sheet on only one side. Furthermore, no spanwise stringer is attached. (See fig. 2.) For the behavior of the transverse end stiffener the following assumptions are made:

1. The deformation of the stiffener in the direction of its own axis is neglected. This assumption is later shown to be permissible.

2. The resistance to bending in the plane of the sheet is neglected in comparison with the corresponding resistance of the sheet. This assumption follows from the fact that $I_{stiffener} << l^3t$, as has been noted previously in reference 8.

Under these assumptions the following boundary conditions hold:

At the built-in end,

$$x = 0, \quad u = 0, \quad v = 0 \qquad (5a,b)$$

At the free end,

$$x = l, \quad \sigma_x = 0, \quad v = 0 \qquad (6a,b)$$

These conditions are those assumed in reference 9. In addition, one condition not previously mentioned is needed to determine the solution numerically. In order to formulate this condition, it is first necessary to determine what may be called the "effective width" of the sheet, that is, that width of the sheet which under the assumption of uniform stress distribution would add the same strength to the beam as the actual sheet under the actual (not yet determined) stress distribution. This width may be written

$$w_{eff}\ (\sigma_x)_{edge} = \int_0^w \sigma_x\ dy \tag{7}$$

If the section modulus W of the beam is determined with this w_{eff}, then the remaining condition is

$$(\sigma_x)_{edge} = \frac{M}{W} \tag{8}$$

In order to determine W, it is first necessary to find the neutral axis of the beam, and then the moment of inertia. The following calculation gives these quantities in a convenient form. For the distance e of the neutral axis from the top one has (fig. 3)

$$e(A_o + w_{eff}t) = e_oA_o \tag{9}$$

The moment of inertia is

$$\begin{aligned} I &= I_o + (e_o - e)^2A_o + e^2w_{eff}t \\ &= I_o + e_o^2A_o + e^2A_o - 2ee_oA_o + e^2w_{eff}t \\ &= I_o + e_o^2A_o + e^2(A_o + w_{eff}t) - 2ee_oA_o \end{aligned}$$

and with (9)

$$\begin{aligned} I &= I_o + e_o^2A_o + ee_oA_o - 2ee_oA_o \\ &= I_o + e_o^2A_o - ee_oA_o \\ &= I_o + ee_o(A_o + w_{eff}t) - e_oA_o \end{aligned}$$

$$I = I_o + ee_ow_{eff}t \tag{10}$$

With (9) and (10) one has

$$\begin{aligned} W = \frac{I}{e} &= \frac{I_o}{e_oA_o}(A_o + w_{eff}t) + w_{eff}t\ e_o \\ &= \frac{I_o}{e_o} + w_{eff}t\left(e_o + \frac{I_o}{e_oA_o}\right) \end{aligned} \tag{11}$$

Introducing (11) into (8) gives

$$(\sigma_x)_{edge}\left[\frac{I_o}{e_o} + w_{eff}t\left(e_o + \frac{I_o}{e_oA_o}\right)\right] = M$$

and with w_{eff} from (7)

$$\frac{I_o}{e_o}(\sigma_x)_{edge} + t\left(e_o + \frac{I_o}{e_o A_o}\right)\int_0^w \sigma_x dy = M$$

$$(\sigma_x)_{edge} + \frac{te_o^2}{I_o}\left(1 + \frac{I_o}{e_o^2 A_o}\right)\int_0^w \sigma_x dy = \frac{e_o}{I_o} M \qquad (12)$$

Equation (12) will serve to make the solution complete.

Introducing the boundary conditions (5) and (6) into the general solution, equations (3) and (4), gives

$$h(y) = 0, \quad k(y) = 0 \qquad (13)$$

$$-lf'(y) + g(y) = 0 \qquad (14)$$

$$\frac{1}{6}l^3 f''(y) - \frac{1}{2}l^2 g'(y) + \left(\frac{E}{G}\right) l\, f(y) = 0 \qquad (15)$$

Inserting (14) into (15) gives

$$-\frac{1}{3}l^3 f''(y) + \left(\frac{E}{G}\right) l\, f(y) = 0 \qquad (16)$$

This second-order linear differential equation has the solution

$$f(y) = c_1 \sinh \kappa y + c_2 \cosh \kappa y \qquad (17)$$

where c_1 and c_2 are constants of integration and

$$\kappa = \frac{1}{l}\sqrt{\frac{3E}{G}} \qquad (18)$$

The stresses are, according to equations (3) and (14)

$$\tau = f(y) \qquad (19)$$

$$\sigma_x = (l - x) f'(y) \qquad (20)$$

Since the normal stress σ_x must be even in y, it follows that

$$c_2 = 0 \qquad (21)$$

The remaining constant c_1 is to be determined from the last edge condition (12). Introducing (20) into (12) gives

$$(l - x)\left[f'(w) + \frac{te_o^2}{I_o}\left(1 + \frac{I_o}{e_o^2 A_o}\right)(f(w) - f(0))\right] =$$

$$= M\,\frac{e_o}{I_o} = P(l - x)\,\frac{e_o}{I_o} \qquad (22)$$

Inserting the value of $f(y)$ from (17) into (22) gives

$$c_1\left[\kappa \cosh \kappa w + \frac{te_o^2}{I_o}\left(1 + \frac{I_o}{e_o^2 A_o}\right)\sinh \kappa w\right] = P \qquad (23)$$

from which one obtains finally for σ_x

$$\sigma_x = \frac{P(l - x)\frac{e_o}{I_o}}{1 + \frac{wte_o^2}{I}\left(1 + \frac{I_o}{e_o^2 A_o}\right)\frac{\tanh \kappa w}{\kappa w}}\;\frac{\cosh \kappa y}{\cosh \kappa w} \qquad (24)$$

It is this expression for σ_x which is to be checked against the experimental data obtained on the symmetrical beam in part II of this report.

THE BEAM WITH ELASTIC END STIFFENER

In this section the extent to which the axial deformation of the end stiffener influences the stress distribution in the sheet is investigated. The result will be that this influence will be so small that the simpler solution of the preceding paragraph is sufficiently accurate under ordinary conditions.

The boundary condition which now must be satisfied – instead of condition (6b), that the transverse end displacement $v(l)$ vanishes – will express the fact that axial deformation of the stiffener under the influence of the shear acting between sheet and stiffener must equal the corresponding deformation of the sheet.

If the transverse-stiffener stress is denoted by σ_s, then, in order that each stiffener element be in equilibrium under the influence of the forces acting on it, one has

$$\frac{\partial}{\partial y}(A_s \sigma_s) - t\,\tau(l) = 0 \qquad (25)$$

The stress σ_s produces an axial strain of amount

$$\epsilon_s = \left(\frac{\partial v}{\partial y}\right)_s = \frac{\sigma_s}{E} \tag{26}$$

For reasons of continuity, $v_s(y)$ must equal the transverse displacement $v(l,y)$ of the sheet. Thus, combining (25) and (26), there follows a condition, containing only sheet stresses and strains

$$\frac{\partial}{\partial y}\left[EA_s \frac{\partial v(l,y)}{\partial y}\right] - t\tau(l,y) = 0 \tag{27}$$

Since no forces are introduced at the free ends of the stiffener, it follows that

$$\sigma_s(w) = E\left(\frac{\partial v(l,y)}{\partial y}\right)_w = 0 \tag{28}$$

All boundary conditions are now represented by (5a,b), (6a), (27), (28), and (12). As before, it follows from (5a,b) and (6a) that in the general solution (3) and (4)

$$h(y) = 0, \quad k(y) = 0 \tag{13}$$

$$g(y) = lf'(y) \tag{14}$$

With that,

$$\tau = f(y) \tag{3b}$$

and from (4b),

$$E\frac{\partial^2 v}{\partial y^2} = \frac{1}{6}x^3 f^{IV}(y) - \frac{1}{2}x^2 g'''(y) + \frac{E}{G}xf''(y) \tag{29}$$

which, with g(y) from (14),

$$E\left(\frac{\partial^2 v}{\partial y^2}\right)_{x=l} = -\frac{1}{3}l^3 f^{IV}(y) + \frac{E}{G}lf''(y) \tag{30}$$

Introducing this relation into the boundary condition (27) gives the differential equation for f(y)

$$-\frac{l^3}{3} f^{IV}(y) + \frac{E}{G} l\, f''(y) - \frac{t}{A_s} f(y) = 0 \tag{31}$$

or

$$f^{IV} - \frac{3E}{G}\frac{1}{l^2} f'' + \frac{3t}{l^3 A_s} f = 0 \tag{31a}$$

Since this is a linear equation containing only derivatives of even order, one may assume for the solution

$$f = \sinh \lambda y \tag{32}$$

which, introduced into (31a), converts this expression into

$$\lambda^4 - \frac{3E}{l^2 G}\lambda^2 + \frac{3t}{l^3 A_s} = 0 \tag{33}$$

$$\lambda^2 = \frac{3E}{2l^2 G}\left[1 \pm \sqrt{1 - \left(\frac{4G^2}{3E^2}\right)\frac{lt}{A_s}}\right] \tag{34}$$

$$\left.\begin{aligned} \lambda_1^2 &= \frac{1}{l^2}\frac{3E}{G}\frac{1}{2}\left[1 + \sqrt{1 - \left(\frac{4G^2}{3E^2}\right)\frac{lt}{A_s}}\right] \\ \lambda_2^2 &= \frac{1}{l^2}\frac{3E}{G}\frac{1}{2}\left[1 - \sqrt{1 - \left(\frac{4G^2}{3E^2}\right)\frac{lt}{A_s}}\right] \end{aligned}\right\} \tag{35}$$

It is remarkable that values of λ_1 and λ_2 are real only so long as

$$\frac{lt}{A_s} < \frac{3}{4}\left(\frac{E}{G}\right)^2 \tag{36}$$

that is, as long as for the given sheet dimensions the stiffener area A_s is not too small. Although there is no great difficulty in handling the cases of complex λ, they are not considered here since the calculations involved would be rather lengthy.

For real λ_1 and λ_2 one has as the solution of equation (31a)

$$f = c_1 \sinh \lambda_1 y + c_2 \sinh \lambda_2 y \qquad (37)$$

The two constants c_1 and c_2 follow from the remaining conditions (28) and (12).

From (28), together with (30),

$$f'''(w) - \frac{3E}{l^2 G} f'(w) = 0 \qquad (38)$$

which gives

$$c_1 \left[\lambda_1{}^3 - \frac{3E}{l^2 G} \lambda_1\right] \cosh \lambda_1 w + c_2 \left[\lambda_2{}^3 - \frac{3E}{l^2 G} \lambda_2\right] \cosh \lambda_2 w = 0 \qquad (39)$$

This can be simplified, observing that from (35) follows

$$\lambda_1{}^2 - \frac{3E}{l^2 G} = -\lambda_2{}^2 \qquad \lambda_2{}^2 - \frac{3E}{l^2 G} = -\lambda_1{}^2 \qquad (40)$$

so that

$$c_1 \lambda_1 \lambda_2{}^2 \cosh \lambda_1 w + c_2 \lambda_2 \lambda_1{}^2 \cosh \lambda_2 w = 0 \qquad (41)$$

With this, (37) becomes

$$f(y) = c_1 \left[\sinh \lambda_1 y - \frac{\lambda_2}{\lambda_1} \frac{\cosh \lambda_1 w}{\cosh \lambda_2 w} \sinh \lambda_2 y \right]$$

and with some other constant, c

$$\tau = f(y) = c \left[\lambda_1 (\cosh \lambda_2 w) \sinh \lambda_1 y - \lambda_2 (\cosh \lambda_1 w) \sinh \lambda_2 y \right] \qquad (42)$$

The normal stress σ_x becomes

$$\sigma_x = (l - x) f'(y)$$

$$= c(l - x) [\lambda_1{}^2 (\cosh \lambda_2 w) \cosh \lambda_1 y - \lambda_2{}^2 (\cosh \lambda_1 w) \cosh \lambda_2 y] \qquad (42a)$$

and the effective width, defined by equation (7)

$$w_{eff} = \frac{\int_0^w \sigma_x dy}{\sigma_x (x,w)} = \frac{(l - x) f(w)}{(l - x) f'(w)}$$

$$w_{eff} = \frac{\lambda_1 \cosh \lambda_2 w \sinh \lambda_1 w - \lambda_2 \cosh \lambda_1 w \sinh \lambda_2 w}{(\lambda_1^2 - \lambda_2^2) \cosh \lambda_2 w \cosh \lambda_1 w}$$

$$w_{eff} = \frac{1}{\lambda_1^2 - \lambda_2^2} [\lambda_1 \tanh \lambda_1 w - \lambda_2 \tanh \lambda_2 w] \qquad (43)$$

In figure 4(a) are plotted values of w_{eff}/w versus w/l for different values of the quantity lt/A_s. These curves, which are taken from reference 1, show that in the practical range, when $0 < w/l < 0.6$, w_{eff}/w is very little influenced by a change or the original assumption $lt/A_s = 0$. It has therefore been considered unnecessary to carry the calculation further toward numerical values for the actual distribution of stress across the panel which was calculated for the case $lt/A_s = 0$.

In reference 1 calculations have also been made taking into consideration the moment of inertia I of the transverse stiffener in the plane of the sheet, which, for equation (43), was assumed equal to zero. Curves corresponding to figure 4(a) have been plotted in figure 4(b) for the limiting case of infinite stiffness $I = \infty$. They also show that, in the practical range, the value of lt/A_s may be considered equal to zero. It may be remarked that the assumption $I = \infty$ is exactly the one to be made if one wants to determine the stresses in a beam built in on two ends and loaded in the middle. For reasons of symmetry the spanwise displacement u is zero along the middle section and one may therefore consider the part of the beam to one side of the middle section as a cantilever with a transverse end stiffener rigid in bending.

D - STRESS DISTRIBUTION IN THE UNSYMMETRICAL BEAM WITH UNSYMMETRICAL LOAD APPLICATION

FORMULATION OF THE PROBLEM

A structure consisting of two side beams of unequal dimensions, and a cover sheet which is attached to both side beams, is to be investigated in this section. The structure is loaded at the free end by two concentrated forces of different magnitudes, each applied to one of the side beams. (See fig. 5.)

There appears to be no previous treatment of this particular structural problem in the literature, whether the shear lag in the cover sheet be considered or disregarded. In order to cover the practical range of structures of this sort a general solution is developed and its application to certain specific arrangements is investigated.

One of the limiting cases for the solution, that for which the sheet width is small compared with the span length so that shear lag is negligible, is derived from the more general solution and the result stated separately.

For the analysis of the structure the following assumptions are made:

1. The distribution of normal stress across the sections of the side beams is linear.

2. The stress distribution in the cover sheet is governed by the laws of plane stress.

DEFINITION OF SYMBOLS

l	span of beam
$2w$	width of beam
I_1, I_2	moments of inertia of side beams
A_1, A_2	cross-sectional areas of side beams
e_1, e_2	distances of neutral axes of side beams from cover
h_1, h_2	heights of side beams
σ_1, σ_2	normal stresses in side beams
τ_1, τ_2	shear stresses in side beams
σ_x, τ	stresses in cover sheet
x, y, z	coordinates: - x,y in plane of sheet, z normal to plane of sheet
b_1, b_2	thicknesses of side beams

P_1, P_2 loads on side beams

$$\gamma = \frac{1}{1 + \frac{I}{e^2 A}}$$

$$\lambda = \frac{tw}{A}$$

$$\alpha = \frac{\coth \mu + \tanh \mu}{\mu}$$

$$\beta = \frac{\coth \mu - \tanh \mu}{\mu}$$

$$\mu = \frac{w}{l}\sqrt{\frac{3E}{G}} = \kappa w$$

BOUNDARY AND OTHER CONDITIONS FOR THE STRESSES

As boundary conditions one has to satisfy the condition of zero shear at the bottom of the side beams:

$$\tau_1(h_1) = 0 \tag{44a}$$

$$\tau_2(h_2) = 0 \tag{44b}$$

the condition that the normal stresses in sheet and side beams are continuous:

$$\sigma_x(-w) = \sigma_1(0) \tag{45a}$$

$$\sigma_x(+w) = \sigma_2(0) \tag{45b}$$

the condition that the edge shear in the sheet is in equilibrium with the shear at the top of the side beams

$$t\,\tau(-w) = -b_1(0)\,\tau_1(0) \tag{46a}$$

$$t\,\tau(+w) = b_2(0)\,\tau_2(0) \tag{46b}$$

As further boundary conditions one has the conditions (5) and (6) at the fixed and at the free end of the sheet, which, as before, give for the sheet stresses

$$\tau = c_1 \sinh \kappa y + c_2 \cosh \kappa y \qquad (19)$$

$$\sigma_x = (l - x)\,\kappa\,[c_1 \cosh \kappa y + c_2 \sinh \kappa y] \qquad (20)$$

In order to complete the statement of the problem, the following equilibrium conditions are added:

The relation between side-beam shear and normal stress,

$$\frac{\partial b(z)\ \tau(z)}{\partial z} + \frac{\partial b(z)\ \sigma(z)}{\partial x} = 0 \qquad (47)$$

which may be integrated - considering (44) - to

$$b_1(z)\tau_1(z) = -\frac{\partial}{\partial x}\int_{h_1}^{z} b_1(z)\sigma_1(z)\ dz \qquad (48a)$$

$$b_2(z)\tau_2(z) = -\frac{\partial}{\partial x}\int_{h_2}^{z} b_2(z)\sigma_2(z)\ dz \qquad (48b)$$

The condition, that the resultant side-beam shear on each side equals the applied load,

$$\int_{h_1}^{0} \tau_1(z)\ b_1(z)dz = P_1 \qquad (49a)$$

$$\int_{h_2}^{0} \tau_2(z)\ b_2(z)dz = P_2 \qquad (49b)$$

On account of the assumed linear normal-stress distribution in the side beams, there may be written

$$\sigma_1 = \sigma_1(0) + z\sigma_1'(0) \qquad (50a)$$

$$\sigma_2 = \sigma_2(0) + z\sigma_2'(0) \qquad (50b)$$

Introducing these expressions into equations (48) for the shear, it follows that

$$\tau_1(z)b_1(z) = -\frac{\partial\sigma_1(0)}{\partial x}\int_{h_1}^{z} b_1(z)dz - \frac{\partial\sigma_1'(0)}{\partial x}\int_{h_1}^{z} zb_1(z)dz \qquad (51a)$$

$$\tau_2(z)b_2(z) = -\frac{\partial\sigma_2(0)}{\partial x}\int_{h_2}^{z} b_2(z)dz - \frac{\partial\sigma_2'(0)}{\partial x}\int_{h_2}^{z} zb_2(z)dz \qquad (51b)$$

and for the shear at the top of beam $(z = 0)$

$$\tau_1(0)b_1(0) = \frac{\partial\sigma_1(0)}{\partial x} A_1 + \frac{\partial\sigma_1'(0)}{\partial x} e_1A_1 \qquad (52a)$$

$$\tau_2(0)b_2(0) = \frac{\partial\sigma_2(0)}{\partial x} A_2 + \frac{\partial\sigma_2'(0)}{\partial x} e_2A_2 \qquad (52b)$$

Introducing equations (51) for the shear into equations (49) gives two equations of the form

$$-\frac{\partial\sigma(0)}{\partial x}\int_h^0 \left\{\int_h^z b(\xi)d\xi\right\}dz - \frac{\partial\sigma'(0)}{\partial x}\int_h^0 \left\{\int_h^z \xi b(\xi)d\xi\right\}dz = P \qquad (53)$$

If one transforms the double integrals in (53), by integration by parts, as follows

$$\int_h^0 \left\{\int_h^z b(\xi)d\xi\right\}dz = \left\{z\int_h^z b(\xi)d\xi\right\}\int_h^0 - \int_h^0 z\, b(z)dz \qquad (54)$$

the part which is integrated out vanishes at both limits, and one obtains instead of (53)

$$-\frac{\partial\sigma_1(0)}{\partial x} e_1A_1 - \frac{\partial\sigma_1'(0)}{\partial x}(e_1{}^2A_1 + I_1) = P_1 \qquad (55a)$$

$$-\frac{\partial\sigma_2(0)}{\partial x} e_2A_2 - \frac{\partial\sigma_2'(0)}{\partial x}(e_2{}^2A_2 + I_2) = P_2 \qquad (55b)$$

The boundary conditions in their final form are now:

1. From (46) and (52),

$$\frac{\partial\sigma_1(0)}{\partial x} + e_1\frac{\partial\sigma_1'(0)}{\partial x} = -\frac{t}{A_1}\tau(-w) \qquad (56a)$$

$$\frac{\partial\sigma_2(0)}{\partial x} + e_2\frac{\partial\sigma_2'(0)}{\partial x} = \frac{t}{A_2}\tau(w) \qquad (56b)$$

2. From (45) and (50),

$$\sigma_1(0) = \sigma_x(-w) \qquad (45a)$$

$$\sigma_2(0) = \sigma_x(w) \qquad (45b)$$

3. Equations (55).

When the sheet stresses $\tau(w)$, $\tau(-w)$, are expressed in terms of $\sigma_x(w)$ and $\sigma_x(-w)$ (or vice versa), one has in equations (55), (56), and (45) six equations for six unknowns, which can be solved.

RELATION BETWEEN EDGE SHEAR AND EDGE NORMAL STRESS IN THE SHEET

The sheet stresses were

$$\tau = c_1 \sinh \kappa y + c_2 \cosh \kappa y \tag{19}$$

$$\sigma_x = (1 - x)\kappa [c_1 \cosh \kappa y + c_2 \sinh \kappa y] \tag{20}$$

If $\sigma_x(w)$ and $\sigma_x(-w)$ are prescribed, one obtains

$$(1 - x)\kappa [c_1 \cosh \kappa w + c_2 \sinh \kappa w] = \sigma_x(w) \tag{57a}$$

$$(1 - x)\kappa [c_1 \cosh \kappa w - c_2 \sinh \kappa w] = \sigma_x(-w) \tag{57b}$$

so that

$$c_1 = \frac{\sigma_x(w) + \sigma_x(-w)}{2(1 - x)\kappa \cosh \kappa w} \tag{58a}$$

$$c_2 = \frac{\sigma_x(w) - \sigma_x(-w)}{2(1 - x)\kappa \sinh \kappa w} \tag{58b}$$

and

$$\tau = \frac{1}{\kappa}\left\{\frac{\sigma_x(w) + \sigma_x(-w)}{2(1 - x)}\,\frac{\sinh \kappa y}{\cosh \kappa w} + \frac{\sigma_x(w) - \sigma_x(-w)}{2(1 - x)}\,\frac{\cosh \kappa y}{\sinh \kappa w}\right\} \tag{59}$$

Writing now

$$\sigma_x = (1 - x)s_x, \quad \sigma_1 = (1 - x)s_1, \quad \sigma_2 = (1 - x)s_2 \tag{60}$$

gives

$$\tau(w) = \frac{1}{\kappa}\left\{\frac{1}{2}[s_x(w)+s_x(-w)] \tanh \kappa w + \frac{1}{2}[s_x(w)-s_x(-w)] \coth \kappa w\right\} \tag{61a}$$

$$\tau(-w) = \frac{1}{\kappa}\left\{-\frac{1}{2}[s_x(w)+s_x(-w)] \tanh \kappa w + \frac{1}{2}[s_x(w)-s_x(-w)] \coth \kappa w\right\} \tag{61b}$$

and the boundary conditions (55), (56), and (45) become

$$s_1(0)\ e_1A_1 + s_1'(0)(e_1^2A_1 + I_1) = P_1 \tag{62a}$$

$$s_2(0)\ e_2A_2 + s_2'(0)(e_2^2A_2 + I_2) = P_2 \tag{62b}$$

$$s_1(0) + e_1s_1'(0) = + \frac{tw}{A_1}\left\{- \frac{s_x(w) + s_x(-w)}{2}\ \frac{\tanh \kappa w}{\kappa w} + \frac{s_x(w) - s_x(-w)}{2}\ \frac{\coth \kappa w}{\kappa w}\right\} \tag{63a}$$

$$s_2(0) + e_2s_2'(0) = - \frac{tw}{A_2}\left\{\frac{s_x(w) + s_x(-w)}{2}\ \frac{\tanh \kappa w}{\kappa w} + \frac{s_x(w) - s_x(-w)}{2}\ \frac{\coth \kappa w}{\kappa w}\right\} \tag{63b}$$

$$s_1(0) = s_x(-w) \tag{64a}$$

$$s_2(0) = s_x(w) \tag{64b}$$

Introducing (64) into (63) and writing for brevity

$$\frac{tw}{A} = \lambda \tag{65}$$

$$\frac{\coth \kappa w + \tanh \kappa w}{\kappa w} = \alpha, \qquad \frac{\coth \kappa w - \tanh \kappa w}{\kappa w} = \beta \tag{66}$$

one obtains

$$s_1(0)\left[1 + \frac{1}{2}\lambda_1\alpha\right] - s_2(0)\left[\frac{1}{2}\lambda_1\beta\right] + s_1'(0)\ e_1 = 0 \tag{67a}$$

$$s_2(0)\left[1 + \frac{1}{2}\lambda_2\alpha\right] - s_1(0)\left[\frac{1}{2}\lambda_2\beta\right] + s_2'(0)\ e_2 = 0 \tag{67b}$$

Eliminating $s_1'(0)$ and $s_2'(0)$ by means of (62):

$$s'(0) = \frac{P}{e^2A + I} - s(0)\frac{eA}{e^2A + I} \tag{62}$$

one has, with the further abbreviation,

$$\frac{1}{1 + \frac{I}{e^2A}} = \gamma \tag{68}$$

$$s_1(0)\left[1+\frac{1}{2}\lambda_1\alpha-\gamma_1\right]-\frac{1}{2}\lambda_1\beta s_2(0)=-\frac{P_1e_1}{e_1{}^2A_1+I_1} \qquad (69a)$$

$$s_2(0)\left[1+\frac{1}{2}\lambda_2\alpha-\gamma_2\right]-\frac{1}{2}\lambda_2\beta s_1(0)=-\frac{P_2e_2}{e_2{}^2A_2+I_2} \qquad (69b)$$

EXPRESSIONS FOR THE STRESSES

Solving the equations (69), one may write:

$$s_1(0)=k_{11}P_1+k_{12}P_2 \qquad (70a)$$

$$s_2(0)=k_{21}P_1+k_{22}P_2 \qquad (70b)$$

where

$$k_{11}=-\frac{\dfrac{e_1}{e_1{}^2A_1+I_1}\left[1+\dfrac{\lambda_2\alpha}{2}-\gamma_2\right]}{\left[1+\dfrac{\lambda_1\alpha}{2}-\gamma_1\right]\left[1+\dfrac{\lambda_2\alpha}{2}-\gamma_2\right]-\dfrac{1}{4}\lambda_1\lambda_2\beta} \qquad (71a)$$

$$k_{12}=-\frac{\dfrac{e_2}{e_2{}^2A_2+I_2}\left[\dfrac{1}{2}\lambda_2\beta\right]}{\left[1+\dfrac{\lambda_1\alpha}{2}-\gamma_1\right]\left[1+\dfrac{\lambda_2\alpha}{2}-\gamma_2\right]-\dfrac{1}{4}\lambda_1\lambda_2\beta} \qquad (71b)$$

$$k_{22}=-\frac{\dfrac{e_2}{e_2{}^2A_2+I_2}\left[1+\dfrac{\lambda_1\alpha}{2}-\gamma_1\right]}{\left[1+\dfrac{\lambda_1\alpha}{2}-\gamma_1\right]\left[1+\dfrac{\lambda_2\alpha}{2}-\gamma_2\right]-\dfrac{1}{4}\lambda_1\lambda_2\beta} \qquad (71c)$$

$$k_{21}=-\frac{\dfrac{e_1}{e_1{}^2A_1+I_1}\left[\dfrac{1}{2}\lambda_1\beta\right]}{\left[1+\dfrac{\lambda_1\alpha}{2}-\gamma_1\right]\left[1+\dfrac{\lambda_2\alpha}{2}-\gamma_2\right]-\dfrac{1}{4}\lambda_1\lambda_2\beta} \qquad (71d)$$

For the fiber stresses at the bottom of the side beams, one obtains, with (62) and (50)

$$s_1(h_1)=s_1(0)+h_1s_1{}'(0)=s_1(0)\left[1-\frac{h_1e_1A_1}{c_1{}^2A_1+I_1}\right]+\frac{h_1P_1}{e_1{}^2A_1+I_1}$$

$$s_1(h_1)=-s_1(0)\frac{(h_1-e_1)e_1}{e_1{}^2A_1+I_1}+P_1\frac{h_1}{e_1{}^2A_1+I_1} \qquad (72a)$$

$$s_2(h_2)=-s_2(0)\frac{(h_2-e_2)e_2}{e_2{}^2A_2+I_2}+P_2\frac{h_2}{e_2{}^2A_2+I_2} \qquad (72b)$$

The distribution of normal stresses across the cover sheet then follows, from (20), (58), (60), and (64), as

$$\sigma_x = (1 - x)\left\{\frac{s_1(0) + s_2(0)}{2}\,\frac{\cosh\kappa y}{\cosh\kappa w} + \frac{s_1(0) - s_2(0)}{2}\,\frac{\sinh\kappa y}{\sinh\kappa w}\right\} \quad (73)$$

Equations (70) to (73) contain the complete result for the problem considered, that of determining the stress distribution for an unsymmetrical beam with unsymmetrical loading.

In the following paragraphs, certain general conclusions which appear to be useful have been drawn.

A CONDITION FOR SYMMETRY OF THE STRESS IN THE SHEET

The condition for symmetry of stress in the sheet is

$$s_1(0) = s_2(0)$$

which by means of (71) may be written

$$P_1 = P_2\,\frac{k_{22} - k_{12}}{k_{11} - k_{21}} \quad (74)$$

or, explicitly,

$$P_1 = P_2\,\frac{e_2\left[1 + \frac{\lambda_1\alpha}{2} - \frac{\lambda_1\beta}{2} - \gamma_1\right]\left[e_1^2A_1 + I_1\right]}{e_1\left[1 + \frac{\lambda_2\alpha}{2} - \frac{\lambda_2\beta}{2} - \gamma_2\right]\left[e_2^2A_2 + I_2\right]}$$

and with (66) and (68)

$$P_1 = P_2\,\frac{e_2\left[\frac{I_1}{e_1^2A_1 + I_1} + \lambda_1\frac{\tanh\kappa w}{\kappa w}\right]\left[e_1^2A_1 + I_1\right]}{e_1\left[\frac{I_2}{e_2^2A_2 + I_2} + \lambda_2\frac{\tanh\kappa w}{\kappa w}\right]\left[e_2^2A_2 + I_2\right]}$$

$$\frac{P_1}{P_2} = \frac{\frac{I_1}{e_1} + \left[\frac{I_1}{e_1} + e_1A_1\right]\frac{tw}{A_1}\,\frac{\tanh\kappa w}{\kappa w}}{\frac{I_2}{e_2} + \left[\frac{I_2}{e_2} + e_2A_2\right]\frac{tw}{A_2}\,\frac{\tanh\kappa w}{\kappa w}} \quad (75)$$

Condition (75), for symmetrical stress in the cover sheet, should be valuable for the experimental verification of the theory.

THE BEAM STRESSES FOR NO SHEAR LAG

When the ratio between width w and span l is a small number, then shear lag will be negligible and the results of the calculation will be simplified. If $w/l \ll 1$, it follows from (66) that

$$\alpha \approx \frac{1}{(\kappa w)^2} + \frac{4}{3}, \qquad \beta \approx \frac{1}{(\kappa w)^2} - \frac{2}{3} \tag{66a}$$

and the equations given previously may be used

$$s_1(0) = k_{11}P_1 + k_{12}P_2 \tag{70a}$$

$$s_2(0) = k_{21}P_1 + k_{22}P_2 \tag{70b}$$

It is somewhat difficult to obtain the limiting values of the k's for α and β approaching infinity because the quantities occur in the combination $\alpha\gamma$, and $\gamma = tw/A$ may approach zero (for instance if the case of two separate beams - cover sheet thickness $t = 0$ - shall be included). Under such circumstances the computation proceeds as follows:

$$k_{11} = -\frac{\dfrac{e_1}{e_1{}^2A_1 + I_1}}{1 - \gamma_1 + \dfrac{\lambda_1}{2}\left[\alpha - \dfrac{(1/2)\lambda_2\beta^2}{1 - \gamma_2 + \alpha\,\lambda_2/2}\right]}$$

$$= \frac{\dfrac{e_1}{e_1{}^2A_1 + I_1}}{1 - \gamma_1 + \dfrac{\lambda_1(1 - \gamma_2)\alpha + (1/2)\lambda_2(\alpha^2 - \beta^2)}{2(1 - \gamma_2) + (1/2)\lambda_2\alpha}} \tag{76}$$

From (66a) follows

$$\alpha^2 - \beta^2 \approx \left[\frac{1}{(\kappa w)^2} + \frac{4}{3}\right]^2 - \left[\frac{1}{(\kappa w)^2} - \frac{2}{3}\right]^2 \approx \frac{8}{3}\,\frac{1}{(\kappa w)^2} + \frac{4}{3}\,\frac{1}{(\kappa w)^2} = \frac{4}{(\kappa w)^2} \approx 4\,\alpha \tag{66b}$$

so that

$$k_{11} = \frac{\dfrac{e_1}{e_1{}^2A_1 + I_1}}{\dfrac{I_1}{e_1{}^2A_1 + I_1} + \dfrac{\lambda_1\alpha}{2}\,\dfrac{(1 - \gamma_2) + 2\,\lambda_2}{(1 - \gamma_2) + \alpha\lambda_2/2}} \tag{77}$$

for $t = 0$ and α finite, that is, with no cover sheet, it follows that

$$k_{11} = -\frac{e_1}{I_1} \tag{78}$$

which is as it should be.

If $t \neq 0$, it is necessary to decide upon a useful range of values for $\lambda\alpha$, which is

$$\lambda\alpha \approx \frac{tw}{A}\left(\frac{l}{w}\right)^2 \frac{G}{3E} = \frac{tl}{A}\left(\frac{l}{w}\right)\frac{G}{3E} \tag{79}$$

Taking as reasonable values $\frac{l}{w} = 10$, $\frac{G}{3E} = \frac{2}{15}$, $A = 20\times0.1$, $t = 0.05$, $l = 200$, one obtains the result, $\lambda\alpha \approx 5\times10\times\frac{2}{15} \approx 6$, which is somewhat larger than γ. Therefore,

$$t \neq 0: \quad k_{11} \approx -\frac{\dfrac{e_1}{e_1{}^2A_1 + I_1}}{\dfrac{I_1}{e_1^2 A_1 + I_1} + \dfrac{A_2}{A_1}\left[\dfrac{I_2}{e_2{}^2A_2 + I_2} + \dfrac{2tw}{A_2}\right]} \tag{80}$$

In this formula it is not correct to make t approach zero in order to obtain the result for the case of the two separate side beams. That result is, however, obtained if t and A_2 are both assumed equal to zero.

For k_{12}, one obtains in the same way from (71b)

$$t = 0: \quad k_{12} = 0$$

$$t \neq 0: \quad k_{12} \approx -\frac{\dfrac{e_2}{e_2{}^2A_2 + I_2}\;\dfrac{1}{2}\lambda_2\,\beta}{(1 - \gamma_1)\dfrac{\lambda_2\alpha}{2} + (1 - \gamma_2)\dfrac{\lambda_1\alpha}{2} + \dfrac{\lambda_1\lambda_2\alpha^2}{4} - \dfrac{\lambda_1\lambda_2\beta^2}{4}} \tag{81}$$

which with (66b) may be written

$$k_{12} \approx - \frac{\dfrac{e_2}{e_2{}^2A_2 + I_2}\,\dfrac{1}{2}\,\lambda_2\beta}{(1 - \gamma_1)\,\dfrac{\lambda_2\alpha}{2} + (1 - \gamma_2)\,\dfrac{\lambda_1\alpha}{2} + \lambda_1\lambda_2\alpha}$$

and since $\alpha \approx \beta$

$$k_{12} \approx - \frac{\dfrac{e_2}{e_2{}^2A_2 + I_2}}{(1 - \gamma_1) + \dfrac{\lambda_1}{\lambda_2}(1 - \gamma_2) + 2\lambda_1} \tag{82}$$

Rewriting equation (82) with, according to (68),

$$1 - \gamma = \frac{I}{e^2A + I} \tag{68a}$$

one has, with (70) and (60), for the normal stress in the top fiber of the side beam which carries P_1

$$\sigma_1 = (l - x)\left\{P_1 \frac{e_1}{I_1 + I_2\dfrac{A_2}{A_1}\,\dfrac{e_1{}^2A_1 + I_1}{e_2{}^2A_2 + I_2} + 2tw\,\dfrac{e_1{}^2A_1 + I_1}{A_1}}\right.$$

$$\left. + P_2 \frac{e_2}{I_2\dfrac{A_2}{A_1} + I_1\,\dfrac{e_2{}^2A_2 + I_2}{e_1{}^2A_1 + I_1} + 2tw\,\dfrac{e_2{}^2A_2 + I_2}{A_1}}\right\} \tag{83}$$

A corresponding result holds for σ_2. Assuming P_2, A_2, t or P_1, A_1, t equal to zero yields the result for two separate side beams.

THE SYMMETRICALLY DEFLECTED BEAM

In a previous section a condition was derived insuring a distribution of stress in the cover sheet symmetrical about the center line $(y = 0)$ of the sheet. It is apparent that for unequal side beams this condition will, in general, produce unequal deflections of the side beams. Since the condition of equal deflection of the two side beams is also of some interest, it shall now be derived.

According to equation (50), the stresses in the side beams are

$$\sigma_1 = \sigma_1(0) + z\ \sigma_1'(0) \tag{50a}$$

$$\sigma_2 = \sigma_2(0) + z\ \sigma_2'(0) \tag{50b}$$

where $\sigma(0)$ and $\sigma'(0)$ are independent of z.

The curvature, and with that the deflection, of the side beams is proportional to the part of the stresses varying linearly with z. Therefore, the condition for equal deflection is,

$$\sigma_1'(0) = \sigma_2'(0) \tag{84}$$

or with (60)

$$s_1' = s_2' \tag{84a}$$

Equations (62) gives s' in terms of s and P

$$s_1' = \frac{P_1}{e_1{}^2 A_1 + I_1} - s_1 \frac{e_1 A_1}{e_1{}^2 A_1 + I_1} \tag{85a}$$

$$s_2' = \frac{P_2}{e_2{}^2 A_2 + I_2} - s_2 \frac{e_2 A_2}{e_2{}^2 A_2 + I_2} \tag{85b}$$

If P_1 and P_2 are introduced from equations (69), there follows

$$-\frac{1}{e_1}\left\{s_1\left[1 + \frac{\lambda_1\alpha}{2} - \gamma_1\right] - s_2\frac{\lambda_1\beta}{2}\right\} - s_1\frac{\gamma_1}{e_1}$$

$$= -\frac{1}{e_2}\left\{s_2\left[1 + \frac{\lambda_2\alpha}{2} - \gamma_2\right] - s_1\frac{\lambda_2\beta}{2}\right\} - s_2\frac{\gamma_2}{e_2}$$

which simplifies to

$$-\frac{s_1}{e_1}\left[1+\frac{\lambda_1\alpha}{2}\right]+\frac{s_2\lambda_2\beta}{2e_1}=-\frac{s_2}{e_2}\left[1+\frac{\lambda_2\alpha}{2}\right]+\frac{s_1\lambda_1\beta}{2e_2}$$

$$s_1\left[\frac{1+\frac{\lambda_1\alpha}{2}}{e_1}+\frac{\lambda_2\beta}{2e_2}\right]=s_2\left[\frac{1+\frac{\lambda_2\alpha}{2}}{e_2}+\frac{\lambda_1\beta}{2e_1}\right] \tag{86}$$

From (69) follows for the relation between P_1 and P_2

$$\frac{P_1}{P_2}\,\frac{e_1}{e_2}\,\frac{e_2^2A_2+I_2}{e_1^2A_1+I_1}=\frac{\left(1+\frac{\lambda_1\alpha}{2}-\gamma_1\right)-\frac{\lambda_1\beta}{2}\left[\frac{s_2}{s_1}\right]}{\left[\frac{s_2}{s_1}\right]\left(1+\frac{\lambda_2\alpha}{2}-\gamma_2\right)-\frac{\lambda_2\beta}{2}} \tag{87}$$

where the ratio $[s_2/s_1]$ is given by equation (86). It would be possible to substitute explicitly (86) into (87). However, the resulting equation would be rather unwieldy, so it seems best to leave the result in the present form.

PART II - EXPERIMENTAL INVESTIGATION

A - SYMMETRICAL BEAM

Description of Test Specimen

In order to confirm or disprove the stress distributions in the corrugated cover sheet indicated by the expressions developed for the symmetrical box beam in section C of part I, a beam was constructed as shown in figures 6 and 7. The side beams were 9 feet 6 inches long and were made from 4-inch, 24ST aluminum-alloy H-beams having 4-inch by 1/4-inch cover plates bolted to them on the sides opposite the corrugated sheet. The corrugated sheet was nominally $1\frac{1}{4}$ by 3/8 inch 24ST aluminum alloy 8 feet 6 inches long by $35\frac{5}{16}$ inches wide. A 4-inch width on each side of the sheet was left flat so that it could be attached to the side beams. The attachment was made by 3/8-inch diameter steel machine bolts spaced 4 inches apart in two rows and staggered to give an effective pitch of 2 inches. The beam was designed to be loaded so that the corrugated cover sheet would be on the tension side of the section.

Figures 8 to 11 show the size of the various members in the test beam in detail. Aluminum-alloy channels were used between the webs of the H-beams at each end and at the center to prevent the beams' rotating under the stresses due to bending. These channels were 2 $^1/_2$ inches deep.

In addition, transverse stiffeners were attached to the beam flanges and to the corrugated sheet at the center of the span and near each end of the sheet to prevent transverse straining of the sheet at these sections. The stiffeners at midspan were very rigid, being two 3-inch structural-steel channels. Two sizes of 24ST aluminum-alloy angles were used for end stiffeners, one being heavier than would be normally employed, the other lighter, in order to demonstrate whether or not a variation in transverse stiffness would materially affect the stress distribution across the corrugated sheet. These stiffeners were attached to the crest of each corrugation by 1/4-inch diameter steel machine bolts and to the flanges of the H-beams by 3/8-inch bolts. The heavier stiffener was a 3 by 2 by 7/16-inch angle having about three times the cross-sectional area of the lighter, which was a 2 by 2 by 3/16 inch. Both were 24ST aluminum-alloy and both were attached by the 2-inch leg; so their spanwise stiffnesses were as nearly the same as they could be made with standard sections of different area.

Methods of Applying Loads and Measuring Strains

Figure 7 shows the beam in the testing machine. Four jacks, one under each end of each of the H-beams, were individually actuated by ratchets and screws to apply the load. The transverse yoke at midspan was attached to the lever system and counterpoise of the balance, permitting the load to be read to 5 pounds.

Spirit levels were placed longitudinally near the center and transversely at each end of the beams to keep them level and equalize the deflection of each side when the jacks were operated. As a further check on the symmetry of loading, 8-inch Berry strain gages were attached to the upper flanges of the H-beams near midspan. These gages are clearly shown in figure 7.

In order to obtain data on the distribution of normal stress across the corrugated sheet at representative points, three transverse sections were explored with Huggenberger tensometers. One, as close to the midspan section of the specimen as it was convenient to work, was $9\,^{1}/_{2}$ inches from the center of the specimen, a second was $11\,^{1}/_{2}$ inches from the end of the beams, or as close to the end of the corrugated sheet as it was convenient to operate the gages. The third section was approximately midway between these two. Because of an observed dissymmetry of strain about the longitudinal center line of the specimen - presumably an axis of symmetry - at this section, a fourth section at a corresponding distance on the other side of the transverse center line was also investigated. Eight Huggenberger tensometers were mounted at each of these sections, their position in each of the four sections being shown in figure 12. Figure 13 indicates the method of attaching the gages through a forked yoke that was, in turn, held to brass hooks by rubber bands. The brass hooks were attached to the corrugated sheet by De Khotinsky cement of medium hardness and Scotch cellulose tape.

Since some trouble was experienced in obtaining good adhesion of the brass hooks to the sheet, especially when the temperature in the laboratory exceeded 80° F, the procedure finally adopted will be described in detail. The sheet and the hooks were thoroughly cleaned with carbon tetrachloride after which the brass hook was heated sufficiently in a Bunsen burner flame that a layer of cement could be melted and spread over the concave surface which was to be in contact with the corrugated sheet. Only a thin layer was used and the hook was put in place on the corrugated sheet before the cement was solidified. In order to obtain a good bond with this cement, it is necessary that both metallic surfaces be hot enough to assure melting of the cement and this temperature was manifestly not attained during this step of the procedure. Three strips of tape, the first about 3 inches long, the second about $2^{1}/_{4}$ and the third about $1^{1}/_{4}$ inches long, were laid over the hook and stuck down, the longest one being stuck to the corrugated sheet and having sufficient adhesion to keep the hook from moving during subsequent operations. These operations involved heating the corrugated sheet from the under side to obtain a bond with the cement previously applied to the hook, the spreading of a further layer of cement over tape and hook, and bonding it to the heated corrugated sheet. With a little practice, skill in manipulating the cement was developed and good bonds were obtained. Care had, of course, to be taken not to heat the aluminum-alloy sheet sufficiently at any point to nullify the effect of the heat treatment or to burn the cement.

During the first series of runs the rubber bands attaching the yokes to the hooks were heavy and exerted a greater force than was necessary to obtain good bearing of the knife edges of the Huggenberger tensometers against the sheet. Lighter bands were subsequently used with satisfactory results and with less trouble caused by pulling the brass hooks from the sheet.

Since but one transverse section could be investigated at a time because of the limited number of gages available, it was necessary to keep the stresses in the sheet well below the yield point of the material. In order to insure that the yield point would not be exceeded the total load on the beam was kept down to 8000 pounds. Simultaneous readings of the strain gages at each section were taken at 1000- or 2000-pound intervals during the loading and the unloading of the beam, and the loads were applied by actuating both jacks at either end of the beam in such a way as to keep the readings of the Berry strain gages attached to the flanges of the H-beams equal. It was understood at the beginning of the tests that the factors for the Berry gages used had recently been checked and were all the same, so that equal readings of the gages would indicate equal strains in the two beams. Subsequent checking of the gage factors showed them to differ by from 0.5 to 4 percent, so that the actual load on the beams was not applied symmetrically when the gages indicated equal strains. The errors introduced in this way were, however, smaller than the percentage difference in gage factors, as the sheet tended to transmit load from one beam to the other and to equalize the deflection of both sides when they were loaded to obtain equality in gage readings.

Table I gives the constants for the gages used, the variation between the constants for calibrations before and after the tests were run being small.

Deviations between Theoretical and Test Beams

Perhaps the greatest difference between the theoretical and the test beams lay in the deviation of the corrugated sheet from the ideal. It appears to have been necessary, when the sheet was formed, to carry the corrugations to one edge and then remove them although this method was not required on both sides of the sheet. This procedure resulted in the metal in one of the 4-inch flat edges used to attach the cover sheet in the side beams having been worked when the sheet was corrugated and reworked when it was flattened; so the sheet as finally delivered had a slight but persistent buckle which could be straightened out in the vicinity of the transverse stiffeners but not between. Because of the facts that six months were required for the forming and delivery of this one sheet, that the time available for conducting the tests was limited, and that no guarantee could be given that a second sheet would be better than the first, the sheet was used on both symmetrical and unsymmetrical beams, care being exercised in fabricating the beams to have the sheet as flat as it could be made. It is believed that any member using a corrugated sheet of these dimensions would have at least as great a deviation from the ideal; hence the redistribution of stress as a consequence of the warping of the panel is probably typical of what might be expected in practice.

Although this may be so, it is admittedly an undesirable feature in a laboratory specimen. The buckle, being on the tension side, tends to flatten out under load, to have an effective stiffness less than that of a perfect sheet, and to produce fictitious readings of the tensometers since part of their indicated strain is due to actual stress and part due to straightening of the element between the legs of the gages. The buckle was so small in this sheet, however, that the effect on the strain-gage readings is believed to be very small, probably negligible, but its effect in reducing the moduli of elasticity in tension and shear is wholly indeterminate. The dissymmetry of the stresses about the center line at section B indicates the effect to be present. Tables II and III show the ordinates from the base of H-beam to the crests of the corrugations at the sections studied and with various loads. Changes of ordinate of 0.03 inch are common; 0.08 inch appears to be the maximum.

A further deviation between actual and theoretical beams results from the end stiffener being so located that the point of load application coincides neither with the end of the sheet nor the line of attachment of stiffener to cover sheet. The use of the two transverse stiffeners at midspan also leaves some uncertainty as to the exact end of the "effective" panel. Whether it be taken at midspan or at the point of attachment of transverse stiffener to cover sheet makes a difference in the value of l used in the expression for σ_x, and hence has an effect on the magnitude of the computed stresses. If l

be taken as the distance between lines of bolts attaching transverse stiffeners, it is 47 inches; if between point of application of load to beam and midspan, it is 52 1/2 inches. Both values will be used in subsequent computations to indicate the effect of varying the assumed panel length.

Perhaps the greatest deviation between actual and theoretical beams lies in the effectiveness of the bolts attaching the corrugated sheet and cover plates to the H-beams. No preliminary tests were made to determine the effective EI of the H-beams before the holes were drilled, after the holes were drilled, or after the holes were drilled in both chords and the 1/4-inch cover plates were attached to one. Tests on other structures have demonstrated that 100-percent efficiencies cannot be counted upon in bolted or riveted connections; hence stresses in cover plates and corrugated sheet will not be as great as though they were made integral with the H-beams. It will be shown in the section on the unsymmetrical beam that this effect is considerable, the increase in moment of inertia as a consequence of adding the 1/4-inch cover plates to the H-beams having been found to be about 70 percent of the value computed on the basis of an integral section of the same dimensions. If the same effectiveness of the bolted connection between H-beams and cover sheet were obtained, the discrepancy between experimentally determined stresses near the edges of the cover sheet and the computed stresses would, to a great extent, be explained.

Precision of Results

In the determination of the strains at any section, the Huggenberger tensometers were read to two figures and plots of gage reading against load were made. Straight lines were faired through the plotted points and, since they did not pass through the origin in every case, parallels which did so were drawn. The gage reading corresponding to a given load on the beam was then read from these lines and recorded to three figures. Since they represent faired average curves, any given strain is probably good to the second figure, but the third is doubtful. There are at least two, and in most cases four or five, sets of strain-gage data for each section, each set having been obtained during a separate load application. Where four or more sets of data are available, the average strain is believed dependable to two decimal places, with the third doubtful. At most sections the maximum deviation of any reading from the mean is about 2 percent, though it is considerably greater at some of the lightly stressed sections.

Because it required 6 months to procure the corrugated cover sheet from the manufacturer, it has been necessary to retain the sheet in an undamaged form for use on the unsymmetrical beam and it has not been possible to obtain Young's modulus for the sheet. In the computation of the stresses from the strain-gage data the standard value of 10,300,000 pounds per square inch has been used. This value is probably within 2 percent of the actual for the sheet.

Owing to a difference in calibration factors for the gages, some of the stress data are based on the values obtained prior to completion of the tests and some on the later values. In most cases no error is involved, but in some gages there was a difference of 2.3 percent in the factors. If all of these errors were cumulative, an error of about 6 percent would occur in the computed stress, but, since some will be positive while others are negative, the probable error to be expected in the stresses obtained from the strain data is about 3.5 percent.

It is more difficult to estimate the probable discrepancy in the stresses computed from the theory. The gage points were located within ±0.05 inch of the cross section, and the point of application of the load was known within about 0.1 inch; so the arms of the loads were known within 0.15 inch and 11.5 inches, at the outer section, or 0.15 inch in about 43 inches at the inner. The error due to uncertainty in moment arm would thus be from 0.35 to 1.3 percent, depending on the section under consideration. The load itself could be measured to the nearest 5 pounds, involving an error of 0.06 percent in the 8000-pound load used as a basis of the analysis. So it may be stated that the moment at any section is known within about 1.4 percent.

Because of variations in actual dimensions from the nominal values for the sections and because of the fact that the beam was fabricated with bolted connections, it is practically impossible to establish percentage variations in effective I at different sections or to compute the exact location of the neutral axis of the beam at various points along the span. Since these effects cannot be exactly evaluated by computation, no effort has been made to do so, and the computed stress data used in comparing theory and empirical results are, for the symmetrical beam, based upon theoretical I_o and e_o values, the only varying dimension or unit considered being the length of panel.

Computation of Stresses

From equation (24) of part I, the stress parallel to the x-axis at any point y inches from the center of the corrugated sheet is

$$\sigma_x = \frac{\dfrac{Pe_o(l - x)}{I_o}}{1 + \dfrac{wte_o^2}{I_o}\left(1 + \dfrac{I_o}{e_o^2 A_o}\right)\dfrac{\tanh Kw}{Kw}} \; \frac{\cosh Ky}{\cosh Kw}$$

P load applied to beam at each loading point
For 8000-pound total load, $P = 2000$ pounds

l panel length between stiffeners
Two values will be used, namely, $l = 47$ and 52.5 inches

x distance from midspan of beam and section under consideration

$(l - x)$ distance between load point and section under consideration, equals 43.0 inches for section A, 27.5 inches for sections B and E, 11.5 inches for section C

e_o distance from centroid of H-beam and cover plate to centroid of flat portion of corrugated sheet = 2.355 inches

I_o moment of inertia of H-beam and cover plate = 15.51 inches

w one-half developed width of corrugated sheet between edges of H-beam flanges = 16.53 inches

w_p one-half projected width of corrugated sheet = 13.55 inches

t thickness of corrugated sheet = 0.0508 inch

A_o area of H-beam and cover plates = 5.203 inch^2

E modulus of elasticity of corrugated sheet, taken as 10,300,000 pounds per square inch

G modulus of rigidity of corrugated sheet, taken as 3,800,000 pounds per square inch

$$\kappa = \frac{1}{l}\sqrt{\frac{3E}{G}}$$

Figure 14 shows the pertinent dimensions for the beam and cover plates for which the properties are computed below.

Determination of Neutral Axis

$$\begin{aligned}
4.00 \times 0.0508 &= 0.2032 \times 0.0254 = 0.0052 \\
\text{H-beam} &= 4.0000 \times 2.0508 = 8.2032 \\
4.00 \times 0.25 &= \underline{1.0000} \times 4.1758 = \underline{4.1758} \\
A_o &= 5.2032 \qquad A_o e_o' = 12.3842
\end{aligned}$$

$e_o' = \dfrac{12.3842}{5.2032} = 2.3801$ inches from extreme fiber to neutral axis

$e_o = 2.3801 - 0.0254 = 2.3547$ inches from centroid of flat part of corrugated sheet to neutral axis

Determination of I_o

$$\begin{aligned}
0.2032 \times 2.3547^2 &= 1.12666 \\
4.0000 \times 0.3293^2 &= 0.43375 \\
1.0000 \times 1.7957^2 &= \underline{3.22454} \\
Ad^2 &= 4.78495
\end{aligned}$$

$I_{c.g.}$ of 1/4-inch plate = 0.00521

$I_{c.g.}$ of H-beam = $\underline{10.72}$

I_o = 15.5102 inch^4

$$\kappa = \frac{1}{l}\sqrt{\frac{3E}{G}} = \frac{1}{47.0}\sqrt{\frac{3 \times 10.3 \times 10}{3.8 \times 10}} = 0.06068$$

$$\text{or } \frac{1}{52.0}\sqrt{\frac{3 \times 10.3 \times 10}{3.8 \times 10}} = 0.05432$$

$\kappa w = 0.06068 \times 16.53 = 1.0030$; or $0.05432 \times 16.53 = 0.89791$

Observed Stresses

Tables V to VII summarize the strain data obtained. The complete strain data presented in graphical and tabular form may be obtained on loan from the NACA. The values tabulated here represent the strains at each gage station in each section for each test run on the specimen with the heavy end stiffener, and with the light, averaged and converted to stresses on the assumption that the modulus of elasticity of the corrugated sheet was 10,300,000 pounds per square inch. Inasmuch as the Huggenberger tensometers were moved from station to station between runs, the likelihood of instrumental errors being serious at any given point is reduced. In most cases the readings are consistent and satisfactory from the standpoint of precision of measurements, though they yield strains, and therefore stress distributions, which are somewhat erratic when viewed in the light of the theoretical curves shown in figure 15. Points for both the heavy and the light end-stiffener specimens have been plotted in that figure for comparison with the theoretical distribution.

It is obvious from the observed stress data that there is no consistent difference between the values for the specimen with the light end stiffener and that with the heavy. Such differences as occur are small in comparison with the magnitudes of the stresses involved and the results appear to confirm the conclusion, established in the development of the theory, that for specimens of normal dimensions the rigidity of the transverse stiffeners had little effect on the distribution of longitudinal stresses in the cover sheet.

Substitution of the foregoing values for the terms in the expression for σ_x, with values of y taken at 4, 8, 12, and 16.53 inches, gives the values recorded in table IV for the computed stresses at these points in sections A, B, and C for beams having either light or heavy end stiffeners.

It is obvious that the stresses observed at the sections surveyed are all less than the computed values except in the vicinity of the H-beams at section C. Observed stress curves have been faired through the points in figure 15 and a computation of the ratio of the stress at y-distances 0, 4, 8, 12, and 16.53 inches from the center of the sheet to the stress at the center of the sheet is made in table VIII for sections A, B, and E. It is interesting to note that these ratios are in close agreement with the values of cosh κy for the corresponding points used in the computation of the theoretical stresses; hence it appears that the theoretical expression is a close approximation to the shape of the normal stress curve at the more highly stressed sections of the cover sheet. The agreement is not good at section C.

The fact that the observed stresses are consistently below the computed at sections A and B appears to indicate that ineffective connections between cover sheet and H-beams result in lower normal stresses at the edge of the cover sheet; hence lower stresses all the way across the sheet, than would be expected from the theory. The observed edge stresses at both sections A and B are between 78 and 80 percent of the computed values while at the center of the sheet the ratios are 81.5 percent at section A, 87.5 percent at B on the basis of the curves computed for $l = 47.0$ inches.

It is known that connections seldom permit the development of the full theoretical stresses in built-up structures whose parts are joined by bolts or rivets. The fact that the observed stresses at the edge of the sheet at section C are greater than the computed involves no inconsistency in this regard since section C is so close to the free edge of the cover sheet that it is doubtful whether the cover sheet contributes its expected part to the strength of the section. The normal stresses observed near the center at section C are so far below the theoretical that the cover sheet appears to be shirking its part in carrying the load at that section; the H-beam would therefore carry appreciably higher stresses than would be necessary were the sheet fully effective.

Consideration of the fact that all stresses in figure 15 are plotted from the same base line shows that the "lag" at section C is appreciably greater than at A or B. Were the central portion of the sheet at section C more effective, the probability is that the observed stress curve would be flatter and that the observed stresses at gages 1 and 8 would drop below the values computed from the theory. This statement cannot be proved on the basis of the data in hand, but it does appear possible to state without fear of contradiction that the normal stresses developed in a wide, thin sheet near its free edge are, for a beam of this type, considerably less than any present theory would indicate and that, because of this fact, the stresses in the side beams or shear webs would be increased beyond their expected values. This result leads a designer to the conclusion that normal stresses in the flanges of side beams may be appreciably greater than indicated by theory in regions of discontinuities in the cover sheets. It is regretted that strain gages were not mounted on the flanges of the side beams of this symmetrical specimen to indicate whether the stresses in beam flange and adjacent area of cover sheet were identical. Had this information been obtained, a more conclusive statement could have been made as to the efficiency of the bolted connection and as to the magnitude of the overstressing of the H-beams, if any, resulting from the understressing of the cover sheet. Although it is difficult to obtain data of this sort, because of the difficulty arising in the attachment of the strain gage to the beam flange, efforts should be made to procure the necessary strain data whenever tests are made on beams involving elements susceptible to shear-lag effects.

B - THE UNSYMMETRICAL BEAM

Description of Test Specimen

The test beam for the unsymmetrical case was as nearly analogous to that for the symmetrical as possible. An 8-inch, 6.53-pound I-beam was substituted for one of the 4-inch, 4.85-pound H-sections. The beam was built so that the plane of the tension chords of the side beams and of the corrugated sheet would be horizontal in the testing machine. This construction resulted in the mid-depth points of the side beams being at different elevations and the neutral axis of the section not being horizontal. Because both side beams were made to deflect the same amount under load, the stresses developed in the sheet at the two side beams were unequal; so an unsymmetrical shear-lag pattern was developed in the corrugated cover sheet. Of the possible alternatives for the unsymmetrical structure it was decided that this arrangement would best serve as a test of the theory and that it would also involve the least likelihood of errors in the empirical data, since it permitted a less complicated loading system than some of the other arrangements.

Figure 16 shows the system of applying the loads to the unsymmetrical beam, and it also shows clearly the arrangement of side beams and corrugated cover sheet. Because of the difference in depth of the side beams the transverse end channels did not run between web centers of the beams, as was the case with the symmetrical beam. The transverse angle stiffeners at the ends of the corrugated sheet were attached as in the case of the symmetrical section, however, and no differences in stress distribution which might have been attributed to a difference in end-stiffener arrangement were noted. Only the light end stiffeners, the 2 by 2 by 3/16-inch angles, were used on the unsymmetrical specimen tested.

The methods of attaching stiffeners, sheet, and side beams were the same as on the symmetrical specimen, and all except the 8-inch I-beam were the same size in both cases.

The load points were located at the ends of the corrugated sheet, 8 feet 6 inches between centers, and the reactions were applied through a frame bearing on load points on the beams at their midspan points. By a careful location of the link attaching this frame to the weighing device, the load was transmitted to the structure so that equal deflections of the side beams were obtained throughout the tests (table IX).

Method of Applying Load and Measuring Strains

Figure 16 shows the beam in the testing machine and indicates the system of applying loads through four jacks. The lower part of the transverse yoke which provided the reaction is shown in that figure, too, while part of the upper portion appears at the top of figure 17. The link between this transverse yoke and the load-weighing mechanism was adjusted horizontally until the deflections of the mid-depth lines of the side beam webs were the same for any load, within the accuracy obtainable by having a fine wire pass over a steel scale calibrated to 1/100 inch. As a further check on the equality of side-beam deflection under load, spirit levels were used at each end of the specimen. Because the whole structure moved vertically under load, it was impossible, without erecting a scaffolding which would have interfered with the test itself, to obtain a more accurate procedure for insuring equality of deflection of the side beams. Since the level bubbles remained centered when the observed deflections were equal, throughout the loading of the specimen, it is believed that the load was divided between the side beams in proportion to their moments of inertia, as was desired.

In order to obtain data as to the distribution of the normal stress across the sheet, a number of fine-wire strain gages of the Ruge - de Forest type were employed at each of three sections, with Huggenberger tensometers added at the two more highly stressed sections to provide checks on the wire gages. Figures 17 and 18 show the wire gages cemented to the sheet. The hooks for the Huggenberger tensometers are also shown although the instruments were not in place when the photographs were taken. The general scheme for attaching the Huggenberger tensometers was the same as in the case of the symmetrical beam except that Duco cement was used in place of De Khotinsky. It was equally successful.

The fine-wire gages were an adaptation of the Ruge-de Forest gage (reference 11) in which an extra-thin, high-rag-content paper was substituted for the heavier plastic material used in the commercially obtainable gages. Each gage, of which about 120 were made, was composed of approximately 6 inches of 0.001-inch copper-nickel alloy wire manufactured by the Driver-Harris Company under the trade-mark name "Advance." The wire was formed in a W shape, cemented between two sheets of thin paper, and soldered to no. 28 silk-covered, tinned magnet-wire leads on the tools shown in figure 19.

The tools were developed by Mr. W. T. Shuler in order to make possible the production of gages of uniform resistance and practically identical electrical constants when reasonable care was exercised in their manufacture. Each gage was examined visually to determine whether any wires were slack or crossed, and a measurement of its unstrained resistance served as a final check on its accuracy and consistency with the others in the series. About 6 gages an hour were produced by one man with this equipment, and those whose resistance varied by more than ±1.2 ohms from the standard for this set, 146 ohms, were rejected. The completed gages, without their lead wires, were about $1^1/_2$ inches long by 3/8 inch wide, and so flexible that they could be attached to flat or curved structural sections without difficulty.

Figure 20 presents theoretical curves of resistance reading against strain based on the electrical constants of the Wheatstone bridge system and data obtained from a very few gages of the quantity made. Several actual calibration points are plotted on the same chart; they were obtained from a further series of gages picked at random from the quantity made and attached to a cantilever beam which, when subjected to known loads, deflected and produced calculable strains. It is seen that the data obtained from the random choice of several gages used for calibration are uniform and in close accord with the curve obtained from coefficients derived from tests on a limited number of gages; hence one feels that the coefficients for the gages used are constant and that the curve may safely be employed for determining strains from resistance readings. Figure 21 facilitates the use of these curves, the strains in inches per inch being plotted in nomographic form against the readings obtained from the decade box used in the Wheatstone bridge circuit.

About 120 gages were made and found acceptable, and 96 were attached to the test specimen, as shown in figure 17. The procedure used in mounting these gages was to clean the surface to which the gage was to be attached by rubbing it with a rag saturated with a half-and-half acetone-Duco solution. This was found to clean the surface effectively and to give it a priming coat. Both surface and gage were then given heavy coats of acetone-Duco solution and the gage was pressed firmly onto the surface of the specimen. After a short setting interval, the entire gage was given a coating of straight Duco cement and just before the cement had completely hardened, the whole mass was pressed firmly to insure a complete bonding to the surface. A period of 24 hours was then allowed for the cement to harden, after which the gage and its cement were covered with melted "Cerosene" wax to protect them against sudden temperature changes and to retard moisture permeating the cement or paper. The gages were attached on sunny days, when humidity was low, in order to reduce any electrical leakage through moisture in the cement.

Gages were attached to a piece of the 4-inch H-beam and inserted into the electrical circuit so that they would compensate for changes in temperature of the whole specimen, and a cloth was used over the end of the beam to which the gages were attached in order to reduce local temperature effects, which would throw errors into the strain readings.

Precision of Results

In the determination of the strains at the sections to which the wire gages were attached, the precision varies from about 1/4 percent at the highly stressed points to approximately 10 percent at the lowest because the accuracy with which any strain could be measured was to the nearest half unit on the decade box. In the range of stresses covered, a half unit represents an actual strain of 0.00000143 inch per inch and the range of strains measured under an 8000-pound change in load on the specimen varies from 0.000015 inch to 0.00068 inch per inch.

A further error was introduced by some of the gages as they did not return to their initial zero readings when the load was removed. The number of such gages was, however, small and the worst offenders were at the section carrying very small stresses; so the phenomenon does not appear to be due to "creep" in the gage or its attachment. Most of the more highly stressed gages had final zero readings within ±1 unit on the decade box from the inital values, whereas those at the lightly stressed section varied from 1 to 9 units - with several at 2 or 3 units - from their original readings. The data at the lightly stressed section mean so little, however, that it is felt that these errors may be disregarded and that the precision of the strain-measuring devices may be taken at from 1/2 to 1 percent on the two highly stressed sections, the error resulting from the limitation in reading the decade box being doubled to allow for possible variation in the "constant" for any gage.

The precision of the strains measured with the Huggenberger tensometers is the same as for the case of the symmetrical beam, about 2 percent.

In the computation of the stresses, a value of E of 10,100,000 pounds per square inch has been used as an average based on the observed EI values for the two side beams. It was taken as 10,300,000 pounds per square inch for the symmetrical beam. In neither case has the actual E of the material in the corrugated sheet been determined, since further testing was contemplated and it has not seemed advisable to destroy the sheet. The values used are, however, probably within 2 percent of the actual for beams and sheet.

As in the case of the symmetrical specimen, the error in computed stress due to inaccuracy in gage location or load measurement varies from about 0.4 percent at section A to about 1.4 percent at section C. As has been mentioned previously, a value of E based on the behavior of the side beams alone has been used. Standard values of E and G for 24ST alloy have been used for the sheet itself.

In the comparison of the observed and the computed stress data, however, the errors resulting from the foregoing causes are obscured by those produced by local distortion or buckling of the corrugated cover sheet. The observed stresses at points where buckling was apparent show a greater deviation from the computed values, or from observed values at adjacent points, than can be attributed to instrumental errors or to lack of precision of the computations or data. It is therefore believed inadvisable to attempt any estimation of the precision of the results as a whole.

Computation of Stresses

From equations (70) to (73), (86), and (87) of part I, the stress parallel to the x-axis at any point y inches from the center of the corrugated sheet may be determined for given values of the pertinent variables. The solution of the equations is more tedious than in the symmetrical case, though not difficult.

Because of the 20-percent discrepancy between computed and observed stresses on the symmetrical beam and because of the fact that this discrepancy was attributed to the low efficiency of joint between cover sheet and side beams, some of the quantities employed in the computation of stresses on the unsymmetrical beam are based on data tained from preliminary tests of the side beams, with and without cover plates. They are thus somewhere between purely theoretical values dependent upon the geometrical properties of the sections employed and purely empirical values back-figured from tests on the completed test specimen. The procedure will therefore be described in considerable detail.

Transverse bending tests were made on both the 4-inch H-beams and the 8-inch I-beams before any holes were drilled in the flanges, after the holes were drilled, and after the 1/4-inch by 4-inch cover plates were added in order to determine the values of EI of the section. The beams were supported near the ends and loaded at the center; deflections at the center were measured on dial gages and the equivalent EI values determined from the deflections, a correction being made for the deflection due to shear. For the 4-inch H-beam, the EI without cover plate is 112,000,000 pound-inches^2, while it increases to but 142,000,000 pound-inches^2 with the 4-inch by 1/4-inch cover plate added. The I_{xx} of the section used was computed from its actual dimensions to be 10.72 inches^4; hence the effective E was 10,450,000 pounds per square inch. The area of the actual section was 4.10 square inches.

Dividing the EI of the beam with cover plate by 10,450,000 yields 13.6 inches^4 for the I of the combination. The area of the cover plate being 1/4 × 4 = 1.0 square inch, the moment of inertia about the centroid of the combination would be

$$I = I_o + A_o e^2 + \eta A_c (2.125 - e)^2$$

when I_o = 10.72 inches^4

A_o = 4.10 square inches

e = distance between centroid of H-beam and that of the combination

η = efficiency factor for cover plate

A_c = cover-plate area = 1.0 square inch

Then $13.6 = 10.72 + 4.10\, e^2 + \eta A_c (2.125 - e)^2$

By trying various values of η, the value of e may be uniquely determined; and when $\eta = 0.74$, $e = 0.325$ inch. The distance between centroid of beam and cover plate, and the extreme fiber of the beam is then $e_o = 2.325$ inches.

With this value established, it is possible to determine the I of beam and cover plate, and of the 4-inch strip of corrugated sheet which is attached to the flange of the H-beam.

$$A_T = 4 \times 0.0508 + 4.10 + 0.74 \times 1.00 = 5.043 \text{ square inches}$$

$$e_1 = \frac{e_o + (0.0508/2)(A_o + A_c)}{A_T} = \frac{(2.3504)(4.84)}{5.043} = 2.255 \text{ inches}$$

whence

$$I_1 = 136 + (4.84)(0.0954)^2 + (0.2032)(2.255)^2 = 14.679 \text{ inches}^4$$

The above values of e_1 and I_1 are used in the stress determination.

For the 8-inch I-beam the EI of the plain beam was 557,000,000 pound-inches^2, and the I_{xx} determined from the section used was 57.12 inches^4, giving an effective E of 9,750,000 pounds per square inch. With the cover plate added, the EI became 666,000,000 pound-inches^2, indicating an effective I of 68.31 inches^4. The cross-sectional area of the beam having been determined to be 5.45 square inches, the value of e was found to be 0.5 inch, and η = 0.75. The value of e_0 was thus 4.5 inches, A_T = 6.4032 and e_2 became 4.38 inches with I_2 = 72.35 inches^4.

It is interesting to note that the efficiency of the cover plate is, in both cases, about 75 percent, indicating that the bolted connections used did not permit the plate to develop the stresses which the ordinary beam theory would indicate, owing possibly to slip in the connection or to a nonuniformity of stress distribution in the cover plate. It is believed that this phenomenon explains, at least in part, the discrepancy between computed and observed stresses in the case of the symmetrical beam.

In the following pages, stresses are computed for various points in test sections A, B, and C, so that curves may be drawn for comparison with the observed stresses obtained from the strain gages. Two cases are considered; one in which the width w is taken as the developed width between the center of the corrugated sheet and the near edge of the beam flange, 16.53 inches; the other in which w is taken to the centers of the beams, 18.53 inches. In both cases the length of the section is taken as 47 inches, the distance between the center lines of the bolts connecting the transverse stiffeners to the corrugated sheet.

The pertinent quantities for use in the stress equations for case I are given in table X.

In the second case, the width of the cover sheet is taken to the center of the side beams; so the portion considered acting with the side beam and its cover plate is but 2 instead of 4 inches wide. This change modified the A, I, and e values slightly as shown in table XII, which summarizes the pertinent values for use in the stress formulas.

Observed Stresses

Table XIV summarizes the stress data for an applied load of 8000 pounds on the test specimen. Because of the buckles in the corrugated sheet, the strains for the "8000-pound load" are actually obtained by differences between those for loads of 6000 and 14,000 pounds, it having been found that the buckles were considerably reduced under the 6000-pound load so that reasonable agreement between computed and observed stresses could be expected. In the computation of stresses from the measured strains, E was taken as 10,100,000 pounds per square inch, the mean between the effective E values found for the two side beams. Since the beams had two different moduli, and since the corrugated sheet probably had a third, some average or weighted value was mandatory and the above was adopted as reasonable.

The Huggenberger tensometers and most of the fine-wire gages were located on the crests of the corrugations, that is, on the side nearest the neutral axis of the specimen. Some of the fine-wire gages were located in the troughs of the corrugations, as is shown in figure 22 which gives the locus of the gages at each section.

The stresses tabulated above for an 8000-pound increment in load are plotted in figure 23 and a broken line is drawn through the points representing the gages in the wave troughs. It is to be noted that the stress curves computed from equations (70) to (73), (86), and (87), in sections A and B lie for the most part between the stresses indicated by the gages in the trough and those on the crest of the waves. This result should be expected because the theoretical data presuppose a flat sheet lying in the plane of the nodes of the corrugations but having properties equal to those of the corrugated sheet. It was thought that with the load carried by the cover sheet being introduced as shear at the edge of the sheet, the normal stresses at crest and trough would be the same, a fact which was neither proved nor disproved on the symmetrical beam because too few gages were employed to give conclusive data.

On the unsymmetrical specimen, sufficient gages were employed to show that the normal stresses varied between crest and trough, probably because the corrugated sheet assumed essentially the same elastic curve as the side beams so that bending stresses were developed in the sheet.

Gages were not used on both sides of the corrugated sheet at any station; so it is impossible to evaluate the normal stress at the midplane of the sheet. The sheet was so thin that the difference between the surface stress and the midplane stress is believed to be small.

Conclusions and Suggestions for Further Research

On the basis of the data shown in figures 23(a) and 23(b) for sections A and B, it may be concluded that the theory developed in part I of this report is in very close accord with the stress distribution occurring in this corrugated sheet, the agreement being better than that for the symmetrical beam. It must be remembered, however, that a modified EI was used for the side beams in the unsymmetrical specimen and, since the modification was made in the direction which the symmetrical specimen indicated to be necessary, a better agreement was to be expected. Regardless of this fact, the agreement between theoretical and observed stresses on these specimens is such as to substantiate the assumptions and indicate that the methods developed in part I are satisfactory for predicting the effects of shear lag on the distribution of normal stresses in corrugated sheets used as chord members of box beams. It is, of course, impossible to state categorically that the agreement attained on these specimens can be expected in all cases, whether the cover sheet be in tension or compression and whether the range in stiffnesses of the side beams be small or large. Further studies on a number of specimens would be necessary before such a conclusion could be established, but the evidence obtained on these beams indicates that the theoretical development is sound.

It is therefore suggested that the research be extended to cover the following points:

1. Further tests on the same specimens with additional transverse stiffeners.

2. Further tests on a similar specimen with greater variation in stiffnesses of side beams, with the same and with additional transverse stiffeners.

3. Tests on a symmetrical specimen having corrugated chords top and bottom, simulating an actual airplane wing spar. (Such a procedure was

impracticable until the development of the fine-wire strain gage due to cost of equipment and inaccessibility of gages when installed in the beam.)

4. Tests on unsymmetrical specimens having corrugated chords top and bottom.

5. Tests on an actual airplane wing panel with due regard for stresses in ribs and other stiffening members.

6. Extension of the procedure to stiffened flat-sheet panels, and a similar series of tests to exploit its applicability.

Guggenheim Aeronautics Laboratory,
Massachusetts Institute of Technology,
Cambridge, Mass., June 4, 1940.

REFERENCES

1. Katz, Hymen: Investigation in Shear-Lag in Corrugated Wide-Flanged Box-Beams. B.S. Thesis, M.I.T., 1938.

2. Aldridge, John F., Jr.: Stress Distribution in Wide Box-Beams as Given by Shear-Lag Theory. M.S. Thesis, M.I.T., 1939.

3. Amarante, B. M.: Stress Distribution in Wide Box-Beams by Shear-Lag Theory. B.S. Thesis, M.I.T., 1939.

4. Amarante, B. M.: Distribution of Stresses in Wide Box-Beams as Given by Shear-Lag Theory. M.S. Thesis, M.I.T., 1939.

5. von Kármán, Th.: Die mittragende Breite. Beiträge zur technischen Mechanik und technischen Physik, August Föppl, zum siebzigsten Geburtstag, Julius Springer (Berlin), 1924, pp. 114-27.

6. Reissner, E.: Ueber die Berechnung von Plattenbalken. Der Stahlbau, vol. 7, no. 26, Dec. 1934, pp. 206-08.

7. Younger, John E.: Miscellaneous Collected Airplane Structural Design Data, Formulas, and Methods. A.C.I.C., vol. VII, no. 644, Materiél Div., Army Air Corps, 1930.

8. Kuhn, Paul: Stress Analysis of Beams with Shear Deformation of the Flanges. T.R. No. 608, NACA, 1937.

9. Reissner, Eric: On the Problem of Stress Distribution in Wide-Flanged Box-Beams. Jour. Aero. Sci., vol. 5, no. 8, June 1938, pp. 295-99.

10. Ebner, H., and Köller, H.: Ueber den Kraftverlauf in längs- und querversteiften Scheiben. Luftfahrtforschung, Bd. 15, Lfg. 10/11, Oct. 10, 1938, pp. 527-42.

11. Baldwin-Southwark Bulletin 155: SR-4 Bonded Metalectric Strain Gage. Baldwin Locomotive Company, Philadelphia, Penna.

Table I - Check of Gage Factors[1]

Instrument number	Previous calibration factor	Final calibration factor
Huggenberger tensometers		
355	1038	1038
357	1047	1035
358	1030	1010
359	1045	1090
361	1062	1062
362	1064	1064
861	1271	1271
862	1196	1192
1090	985	985
1092	1045	1045
8-inch Berry gages and dials		
86-33	2.0 + 80000	2.010 + 80000
87-24	2.0 + 80000	2.050 + 80000
85-15	2.0 + 80000	2.000 + 80000
88-29	2.0 + 80000	2.080 + 80000

[1]For Huggenberger tensometers, the gage reading must be divided by the gage factor to give the strain in inches per inch. For the Berry and dial gages, the gage reading must be multiplied by the gage factor to give the strain in inches per inch.

Load at center (lb) \ Station	1	2	3	4	5	6	7	8
	Distance (in.)							
Section A								
0	3.89	3.92	3.95	3.97	3.95	3.94	3.91	4.05
4000	3.89	3.92	3.95	3.97	3.96	3.94	3.93	4.05
5500	3.89	3.92	3.95	3.97	3.97	3.94	3.94	4.05
Section B								
0	3.91	3.79	3.92	3.97	3.92	3.81	3.78	4.05
4000	3.91	3.82	3.95	3.99	3.97	3.88	3.83	4.04
5500	3.91	3.83	3.95	3.99	3.97	3.89	3.83	4.05
Section C								
0	3.97	3.88	3.97	3.97	3.94	3.92	3.93	4.03
4000	3.97	3.91	3.95	3.99	3.98	3.97	3.93	4.03
5500	3.97	3.91	3.94	4.00	4.00	3.97	3.94	4.03

Table II - Variation of Distance with Load at Center for Heavy End Stiffener (from crest of corrugation to base of H-beam)

Table III - Variation of Distance with Load at Center for Light End Stiffener (from crest of corrugation to base of H-beam)

Load at center (lb) \ Station	1	2	3	4	5	6	7	8
	Distance (in.)							
Section A								
0	3.87	3.92	3.95	3.95	3.95	3.94	3.91	4.05
4100	3.88	3.92	3.95	3.96	3.95	3.94	3.92	4.06
6100	3.88	3.92	3.94	3.96	3.95	3.94	3.92	4.06
Section B								
0	3.91	3.77	3.89	3.94	3.87	3.89	3.77	4.05
4100	3.91	3.79	3.90	3.94	3.92	3.86	3.81	4.05
6100	3.91	3.79	3.90	3.94	3.92	3.86	3.81	4.06
Section C								
0	3.97	3.81	3.91	3.92	3.89	3.87	3.87	4.03
4100	3.96	3.83	3.92	3.94	3.93	3.91	3.87	4.02
6100	3.96	3.83	3.92	3.94	3.93	3.91	3.87	4.02
Section D								
0	3.86	3.77	3.82	3.88	3.91	3.94	4.00	4.06
4100	3.85	3.78	3.84	3.90	3.91	3.93	3.98	4.06
6100	3.85	3.78	3.84	3.90	3.90	3.92	3.98	4.06

Table IV - Computed Stresses at Test Sections

	Section A		Section B and E		Section C	
K	0.06068	0.05432	0.06068	0.05432	0.06068	0.05432
y	σ_x	σ_x	σ_x	σ_x	σ_x	σ_x
0	6248	6687	3996	4277	1671	1789
4	6435	6846	4114	4378	1720	1831
8	6999	7329	4476	4687	1872	1960
12	7979	8159	5103	5218	2134	2182
16.53	9663	9569	6180	6120	2584	2559

The stresses given in table IV are plotted in figure 15.

Table V - Average Stresses at Section A (based on E = 10,300,000 pounds per square inch)

Heavy End Stiffener

Gage Station	1	2	3	4	5	6	7	8
Developed dist. from center line of sheet, in.	16.14	11.53	6.93	2.31	2.31	6.92	11.53	16.14
Test Run A-1	0.688	-	0.541	0.461	-	-	-	0.803
A-2	.668	-	.541	.466	.488	.569	.602	.801
A-3	.676	.613	.560	.488	.524	.603	.607	.801
A-4	.680	.623	.555	.479	.529	.594	.602	.776
A-5	.714	.628	.541	.451	.494	.560	.584	.767
Sum	3.426	1.864	2.738	2.345	2.035	2.325	2.393	3.948
Average Strain x 10^3 in.	0.6852	0.6213	0.5476	0.4690	0.5088	0.5812	0.5982	0.7896
Stress, lb/sq in.	7050	6400	5640	4830	5240	5990	6160	8130

Light End Stiffener

Gage Station	1	2	3	4	5	6	7	8
Test Run A-18	0.709	0.661	0.549	0.466	0.493	0.551	0.594	0.787
A-19	.687	.635	.534	.423	.502	.546	.584	.760
Sum	1.396	1.296	1.083	0.889	0.995	1.097	1.178	1.547
Average Strain x 10^3 in.	0.698	0.648	0.542	0.445	0.498	0.549	0.589	0.774
Stress, lb/sq in.	7190	6680	5570	4580	5130	5650	6060	7960

Table VI - Average Stresses at Sections B and E (based on E = 10,300,000 pounds per square inch)

Heavy End Stiffener

Gage Station	1	2	3	4	5	6	7	8
Test Run A-6	-	0.387	-	-	0.338	0.294	0.306	-
A-7	.440	.408	-	-	.372	-	.376	-
A-8	.432	.392	.386	.354	.348	.324	.376	.528
A-9	.428	.392	.361	.387	.353	-	-	.528
A-10	.444	.396	.406	.392	.344	.324	.339	.490
A-11	.444	.371	.388	.382	.334	.321	.348	-
A-12	-	.376	.397	.382	.319	.351	.315	.436
A-13	.440	.401	.390	.375	.361	.363	.373	.487
Sum	2.628	3.123	2.318	2.272	2.749	1.977	2.433	2.469
Average Strain x 10^3 in.	0.4380	0.3903	0.3863	0.3787	0.3436	0.3295	0.3476	0.4938
Stress, lb/sq in.	4560	4025	3980	3900	3540	3390	3580	5090

Light End Stiffener

Section B								
Gage Station	1	2	3	4	5	6	7	8
Test Run A-20	0.498	0.427	0.422	0.395	0.338	0.333	0.326	0.496
A-21	.470	.407	.397	.381	.347	.338	.393	.480
Section E								
Test Run A-25	0.461	0.382	0.353	0.329	0,307	0.394	-	0.432
A-26	.433	.361	.371	.353	.377	.400	.421	.482
A-27	.445	.411	.381	.356	.361	.402	.422	.451
Average Stress Sect. B lb/sq in.	4980	4310	4220	4000	3525	3455	3545	5030
Average Stress Sect. E	4580	3960	3790	3560	3690	4100	4340	4680
Average Stress Sects. B and E	4780	4135	4005	3780	3560	3780	3945	4855

Table VII - Average Stresses at Section C (based on E = 10,300,000 pounds per square inch)

Heavy End Stiffener

Gage Station	1	2	3	4	5	6	7	8
Test Run A-14	0.287	0.099	0.071	0.057	0.097	0.083	0.183	-
A-15	.310	.088	.072	.076	.064	.089	.183	.293
A-16	.279	.097	.048	.061	.059	.099	.188	.302
A-17	.268	.092	.070	.070	.076	.074	.182	.295
Sum	1.144	0.376	0.261	0.264	0.296	0.345	0.736	0.890
Average Strain x 10^3 in.	0.2860	0.0940	0.0653	0.0660	0.0740	0.0863	0.1840	0.2967
Stress, lb/sq in.	2950	968	673	680	762	888	1895	3060

Light End Stiffener

Gage Station	1	2	3	4	5	6	7	8
Test Run A-22	0.239	0.108	0.092	0.081	0.108	0.066	0.239	0.256
A-23	.243	.103	.072	.061	.099	.070	.239	-
A-24	.247	.103	.058	.061	.080	.066	.244	-
Sum	0.729	0.314	0.222	0.203	0.287	0.202	0.722	0.256
Average Strain x 10^3 in.	0.2430	0.1047	0.0740	0.0676	0.0957	0.0673	0.2407	0.256
Stress, lb/sq in.	2510	1075	762	696	985	693	2480	2640

Table IX - Comparative Deflections of Side beams

Load (lb)	Deflection at midspan (in.)	
	4-inch H-beam	8-inch I-beam
0	0.000	0.000
2000	.053	.043
4000	.098	.095
6000	.149	.141
8000	.190	.188
10000	.241	.236
12000	.283	.277

Table XI - Computed Stresses

Case I

							Stresses		
							Sect A	Sect B	Sect C
$y_{dev.}$	κy	cosh κy	sinh κy	76.214 x cosh κy	-30.646 x sinh κy		l-x=41.5	l-x=26	l-x=10
16.53	1.0017	1.545	1.178	117.75	36.16	81.59	3386	2121	816
15.00	.9090	1.442	1.040	109.90	31.92	77.98	3236	2027	780
12.00	.7272	1.276	.7858	97.25	24.12	73.13	3035	1901	731
9.00	.5454	1.152	.5739	87.80	17.59	70.21	2914	1825	702
6.00	.3636	1.067	.3716	81.32	11.41	69.91	2901	1818	699
3.00	.1818	1.016	.1829	77.43	5.61	71.82	2980	1867	718
0	0	1.000	0	76.21	0	76.21	3163	1981	762
-3.00	-.1818	1.016	-.1829	77.43	-5.61	83.04	3446	2159	830
-6.00	-.3636	1.067	-.3716	81.32	-11.41	92.73	3848	2411	927
-9.00	-.5454	1.152	-.5729	87.80	-17.59	105.39	4374	2740	1054
-12.00	-.7272	1.276	-.7858	97.25	-24.12	121.37	5037	3156	1214
-15.00	-.9090	1.442	-1.040	109.90	-31.92	141.82	5886	3687	1418
-16.53	-1.0017	1.545	-1.178	117.75	-36.16	153.91	6387	4002	1540

These data are plotted in figure 23 as solid lines.

Table VIII - Comparison of Observed Stress Ratios with Cosh κy

y (in.)	16.53	12	8	4	0	4	8	12	16.53
	Section A								
Observed stress, (lb/sq in.)	7230	6380	5760	5290	5100	5330	5920	6800	8175
S_y/S_o	1.418	1.250	1.130	1.037	1.000	1.045	1.162	1.333	1.604
	Sections B and E								
Observed stress, (lb/sq in.)	4700	4180	3890	3680	3500	3580	3825	4275	5000
S_y/S_o	1.342	1.195	1.110	1.052	1.000	1.022	1.095	1.220	1.430
	Values of Cosh κy for l = 47.0 and l = 52.5 in.								
Cosh κy	1.547	1.277	1.120	1.030	1.000	based on l = 47.0			
Cosh κy	1.451	1.220	1.096	1.024	1.000	based on l = 52.5			

Table X

Case I

$I_1 = 14.679 \text{ in.}^4$ $\quad$ $I_2 = 72.35 \text{ in.}^4$

$A_1 = 5.045 \text{ sq in.}$ $\quad$ $A_2 = 6.4032 \text{ sq in.}$

$e_1 = 2.255 \text{ in.}$ $\quad$ $e_2 = 4.380 \text{ in.}$

$l = 47 \text{ in.}$

$w = 16.53 \text{ in.}$

$\kappa = 0.0606$

$\kappa w = 1.0017$

$\tanh(\kappa w) = 0.7624$

$\coth(\kappa w) = 1.3116$

$$\alpha = \frac{\coth \kappa w + \tanh \kappa w}{\kappa w} = 2.0705$$

$$\beta = \frac{\coth \kappa w - \tanh \kappa w}{\kappa w} = 0.5483$$

$$\gamma_1 = \frac{1}{1 + \frac{I_1}{e_1^2 A_1}} = 0.6360 \qquad \gamma_2 = 0.6293$$

$$\lambda_1 = \frac{tw}{A_1} = 0.16651 \qquad \lambda_2 = 0.13114$$

$$P = P_1 + P_2 = 8000 \text{ lb}$$

Substitution of these values in equations (70) to (73), (86) and (87), yields

$$\frac{s_1(0)}{s_2(0)} = 0.5301$$

$$\frac{P_1}{P_2} = 0.1965$$

$P_1 = 656.9 \text{ lb.}$ $\quad$ $P_2 = 3343.1 \text{ lb.}$

$s_1(0) = -235.49$ $\quad$ $s_2(0) = -153.90$

Table XII

Case II

$I_1 = 14.14 \text{ in.}^4$ $\quad$ $I_2 = 70.34 \text{ in.}^4$

$A_1 = 4.9416 \text{ sq in.}$ $\quad$ $A_2 = 6.3016 \text{ sq in.}$

$e_1 = 2.302 \text{ in.}$ $\quad$ $e_2 = 4.453 \text{ in.}$

$l = 47 \text{ in.}$

$w = 18.53 \text{ in.}$

$\kappa = .0606$

$\kappa w = 1.123$

$\tanh(\kappa w) = 0.7667$

$\coth(\kappa w) = 1.3043$

$$\alpha = \frac{\coth \kappa w + \tanh \kappa w}{\kappa w} = 1.8442$$

$$\beta = \frac{\coth \kappa w - \tanh \kappa w}{\kappa w} = 0.4787$$

$$\gamma_1 = \frac{1}{1 + \frac{I_1}{e_1^2 A_1}} = 0.6494 \qquad \gamma_2 = 0.640$$

$$\lambda_1 = \frac{tw}{A_1} = 0.1905 \qquad \lambda_2 = 0.1494$$

$$P = P_1 + P_2 = 8000 \text{ lb}$$

Substitution of the above values in equations (70) to (73), (86) and (87) yields,

$$\frac{s_1(0)}{s_2(0)} = 0.5307$$

$$\frac{P_1}{P_2} = 0.1949$$

$P_1 = 652.5 \text{ lb.}$ $\quad$ $P_2 = 3347.5 \text{ lb.}$

$s_1(0) = -84.57$ $\quad$ $s_2(0) = -159.35$

Table XIII - Computed Stresses

Case II

							Stresses		
							Sect A	Sect B	Sect C
y dev.	ky	cosh ky	sinh ky	71.75 x cosh ky	-27.211 x sinh ky		l-x=41.5	l-x=26	l-x=10
18.53	1.123	1.700	1.374	121.96	-37.39	84.57	3510	2199	846
15.00	.9090	1.442	1.040	103.45	-28.30	75.15	3120	1954	752
12.00	.7272	1.276	.7858	91.54	-21.38	70.16	2912	1824	702
9.00	.5454	1.152	.5729	82.64	-15.59	67.05	2783	1743	671
6.00	.3636	1.067	.3716	76.55	-10.11	66.44	2757	1727	664
3.00	.1818	1.016	.1829	72.89	-4.98	67.91	2818	1766	679
0.00	0	1.000	0	71.75	0	71.75	2978	1866	718
-3.00	.1818	1.016	-.1829	72.89	+4.98	77.87	3232	2025	779
-6.00	.3636	1.067	-.3716	76.55	10.11	86.66	3596	2253	867
-9.00	.5454	1.152	-.5729	82.64	15.59	98.23	4077	2554	982
-12.00	.7272	1.276	-.7858	91.54	21.38	112.92	4686	2936	1129
-15.00	.9090	1.442	-1.040	103.45	28.30	131.75	5468	3426	1318
-18.53	1.123	1.700	1.374	121.96	37.39	159.35	6613	4143	1594

These data are plotted in figure 23 as dash lines.

Table XIV - Stress Data for 8000-Pound Load on Beam

Section A		Section B		Section C	
Gage No.	Stress (lb.)	Gage No.	Stress (lb.)	Gage No.	Stress (lb.)
H-3	4020	C-9	2680	I-1	-
H-4	3720	C-8	2000	G-11	555
H-5	3730	E-6	1910	F-8	788
A-2	2580	E-7	1690	F-9	1010
A-3	2670	E-8	1830	F-10	152
Hugg 1	1540	Hugg 5	2000	F-11	242
A-4	2730	E-9	2050	G-1	374
A-5	3110	E-10	1910	G-2	858
A-6	2630	E-11	2110	G-3	425
Hugg 2	2300	F-1	1870	G-4	475
A-7	2530	F-2	1730	G-5	950
A-8	3380	Hugg 6	1780	G-6	1870
A-9	2800	F-3	1950	G-7	1305
Hugg 3	3190	F-4	2780	I-5	1540
A-10	3460	F-5	3330	I-4	1980
A-11	4020	G-10	4130		
E-1	4070	G-9	4410		
Hugg 4	3960				
E-2	4780				
E-3	5620				
H-6	—				
H-7	6870				
H-8	6780				

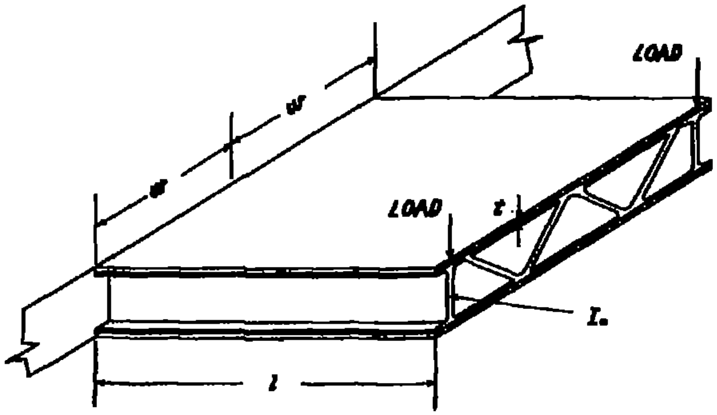

Fig. 1

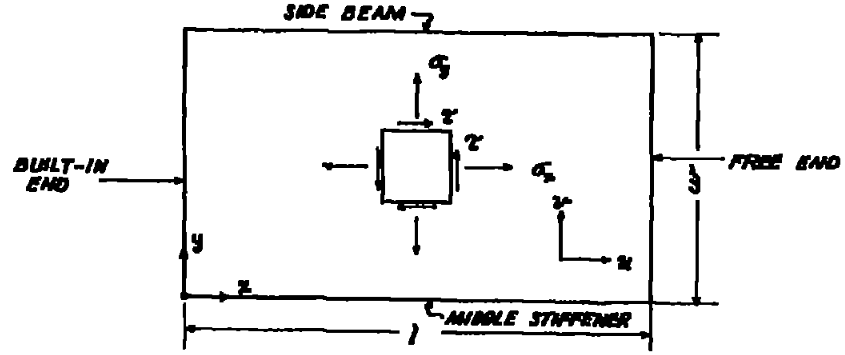

Fig. 2a

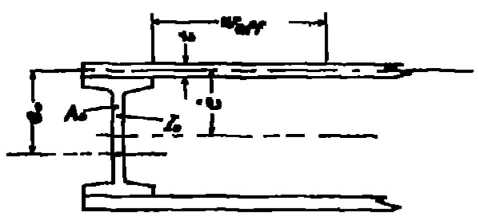

Fig. 3

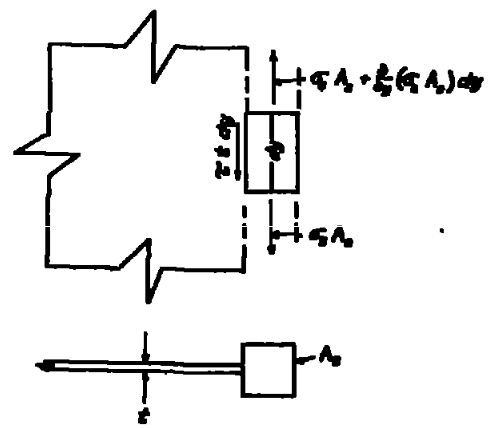

Fig. 2b

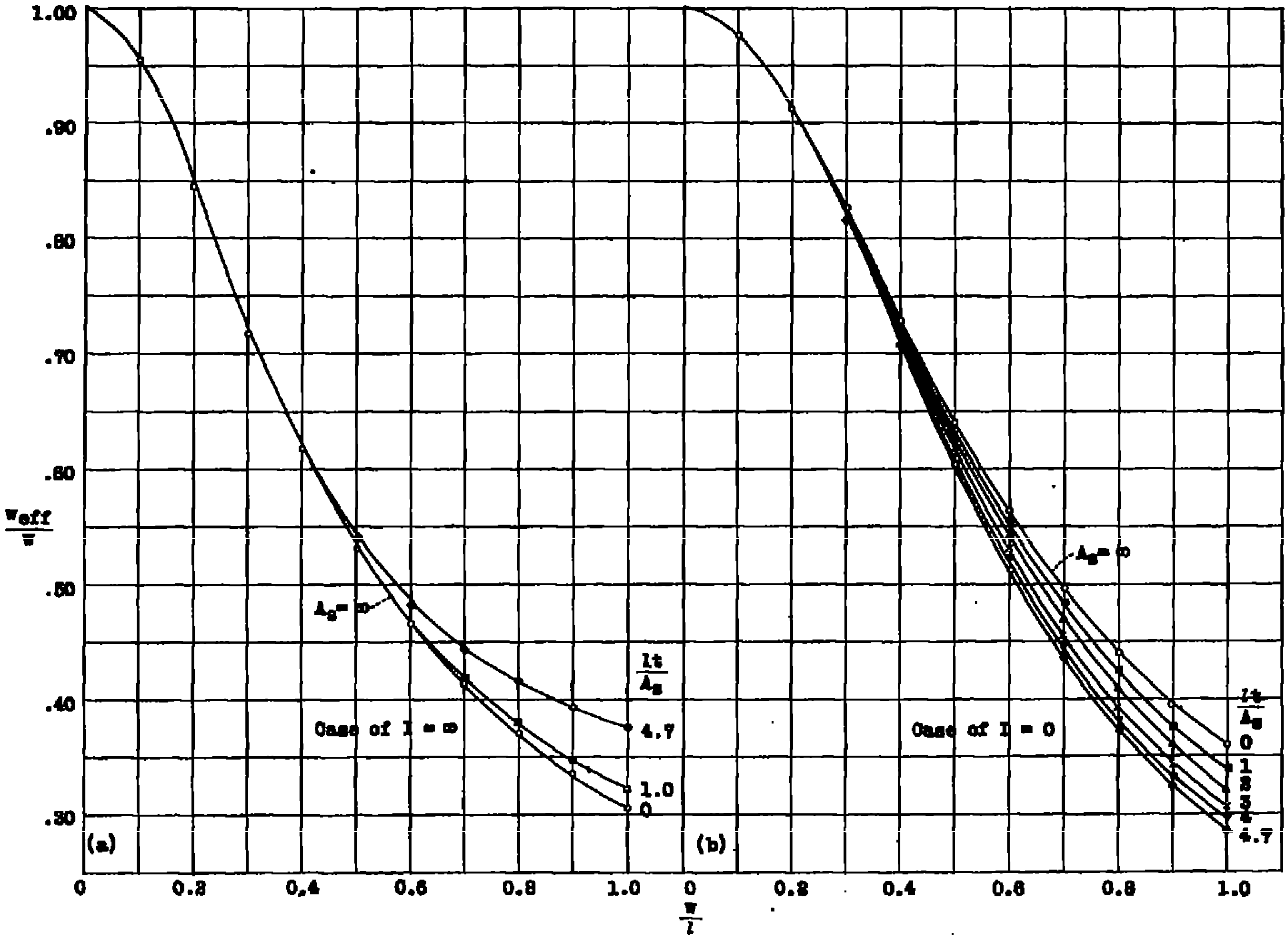

Figure 4.- Variation of $\frac{w_{eff}}{w}$ with $\frac{w}{l}$ for $\frac{lt}{A_s}$ values from 0 to 4.7.

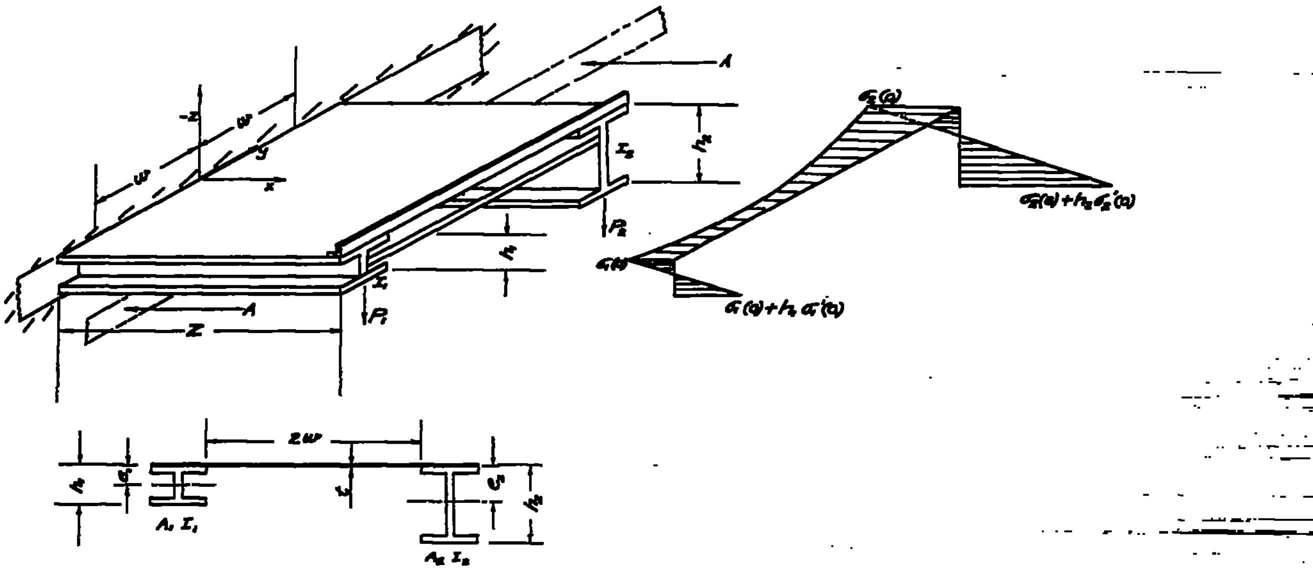

SECT. A-A

FIG. 5

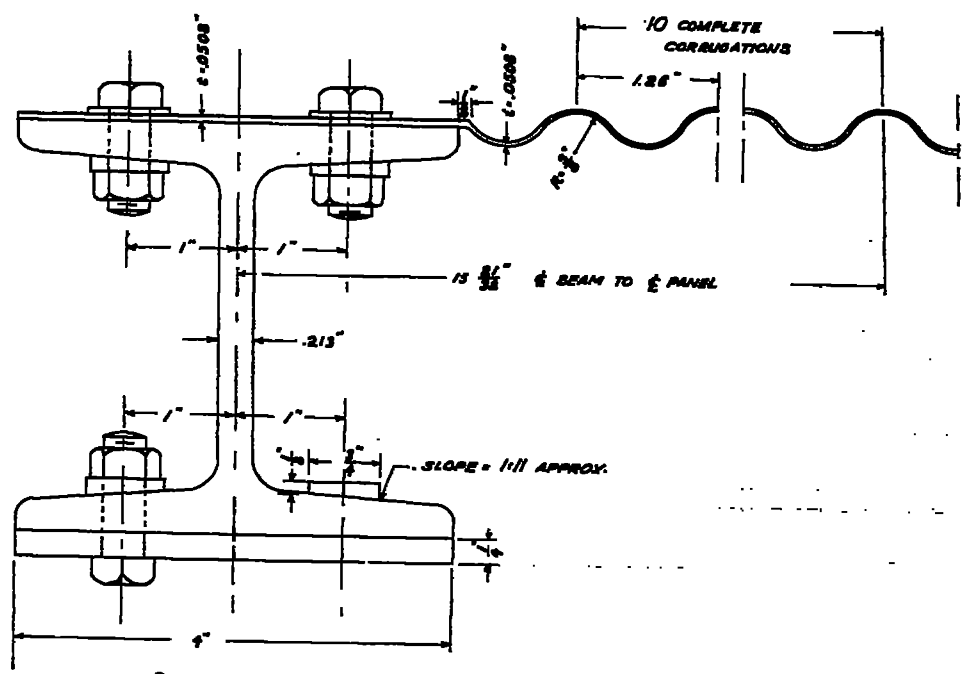

DETAIL SHOWING CONNECTION OF FLANGE TO H-BEAM

FIG. 9

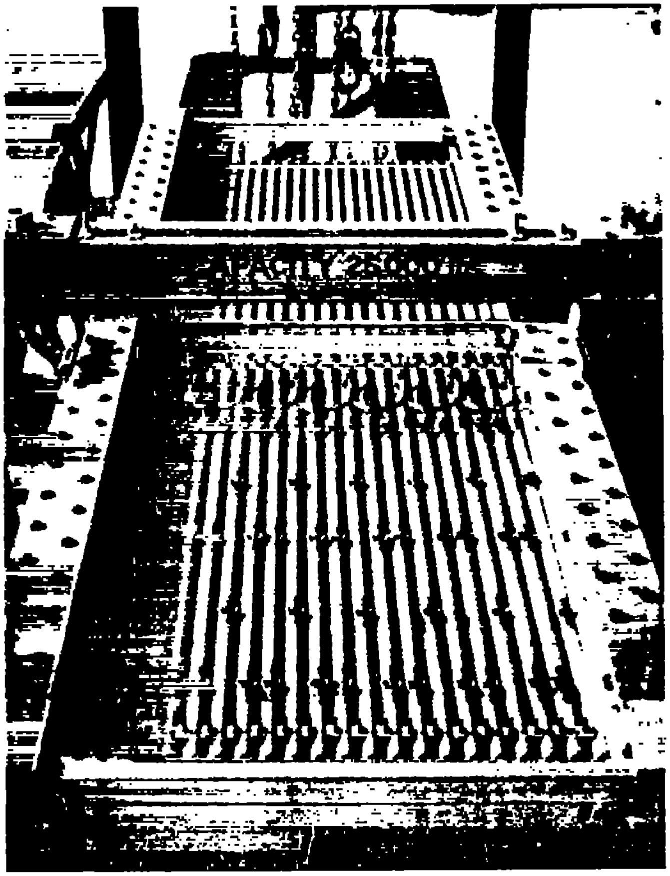

Figure 6.- Test beam as seen from above.

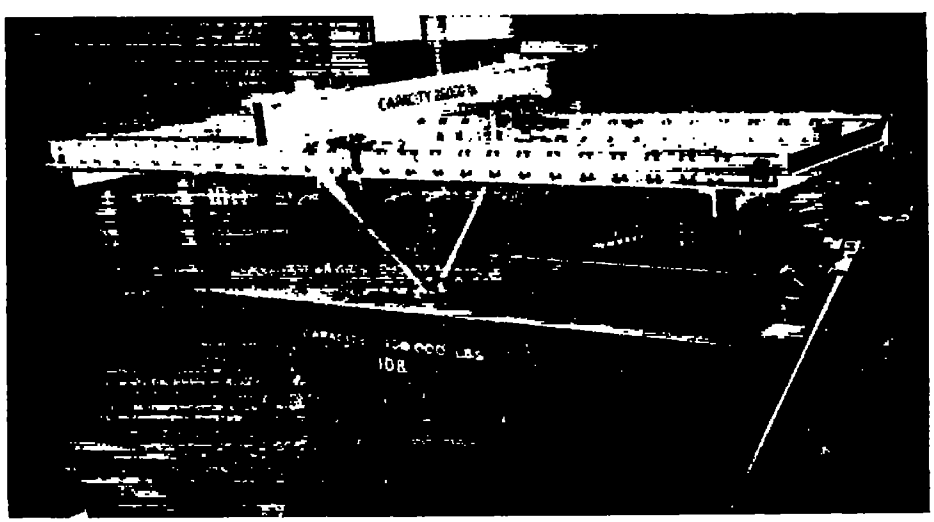

Figure 7.- Beam mounted in testing machine.

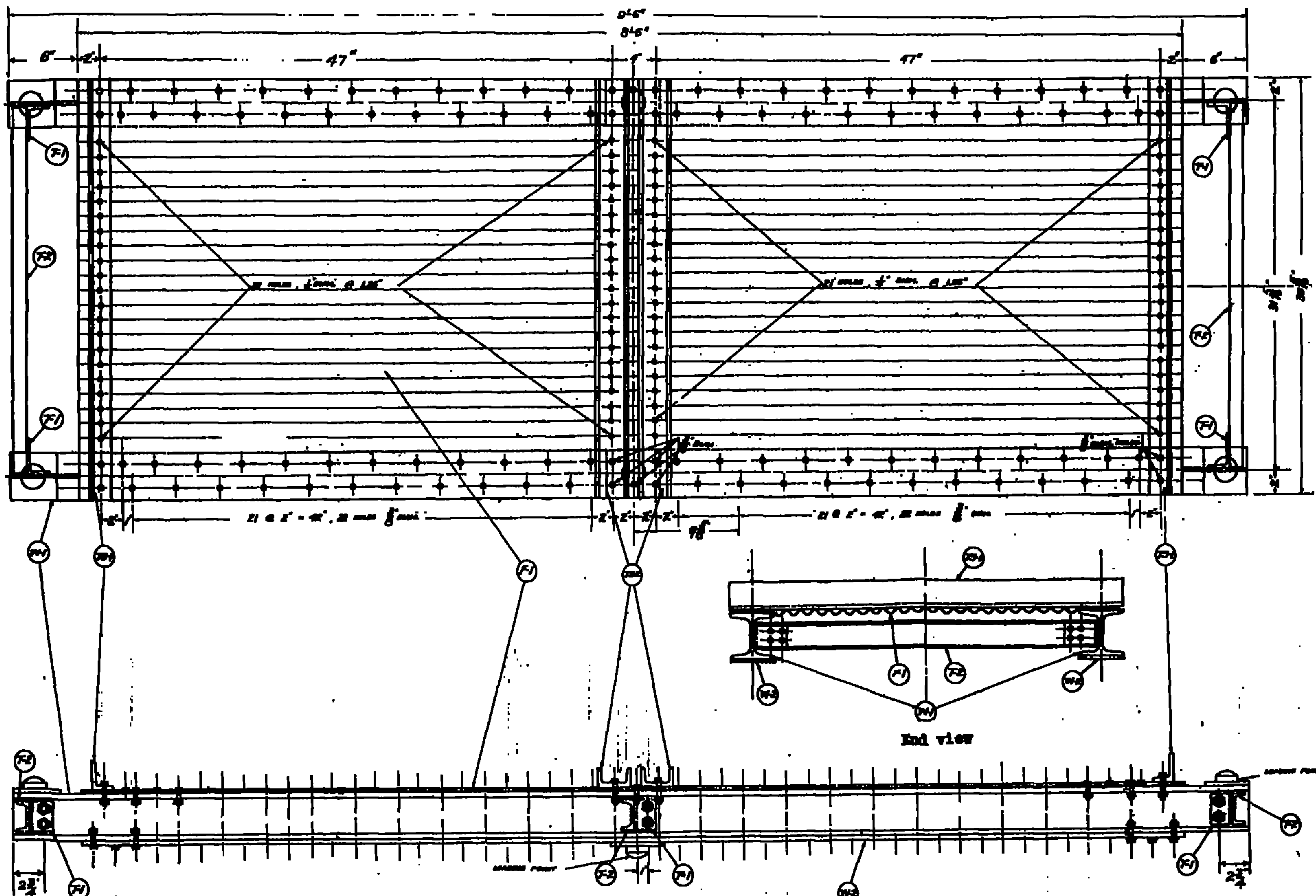

Figure 8.

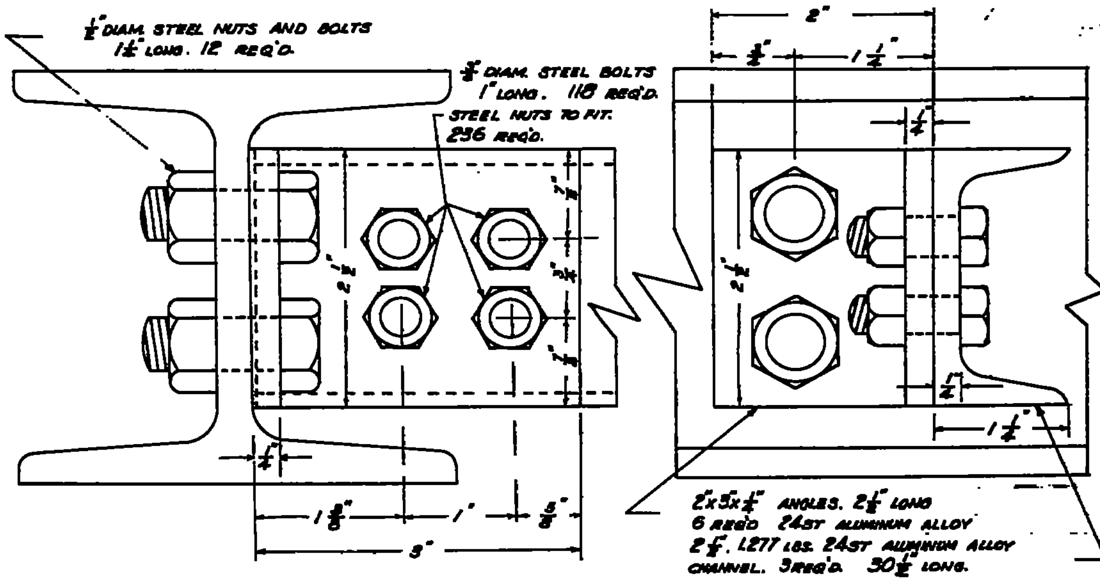

DETAIL SHOWING CONNECTION OF BULKHEADS AT CENTER LINE AND END OF WEBS

FIG. 10

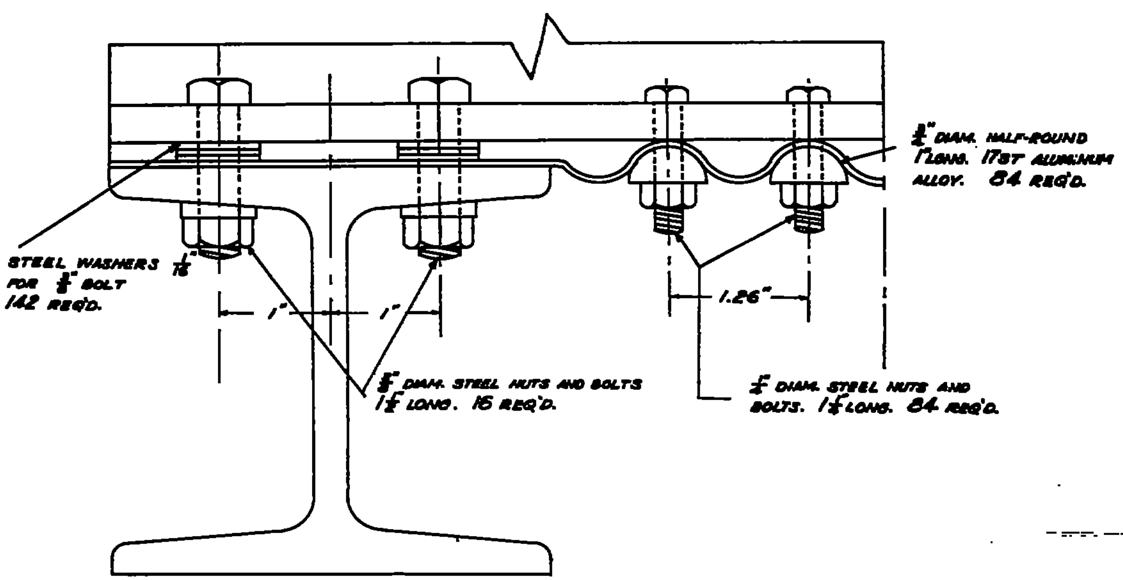

DETAIL SHOWING CONNECTION OF TRANSVERSE STIFFENER TO CORRUGATED FLANGE AND ALUMINUM ALLOY BEAMS.

FIG. 11

SKETCH SHOWING
LOCATION OF STATIONS AND SECTIONS

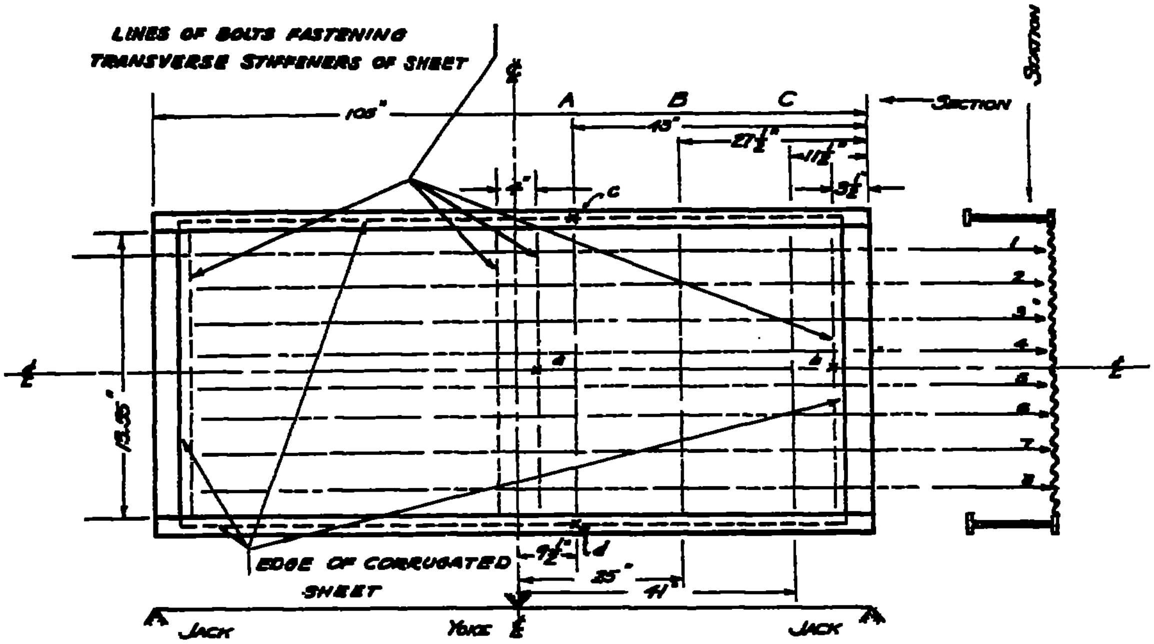

FIG. 12

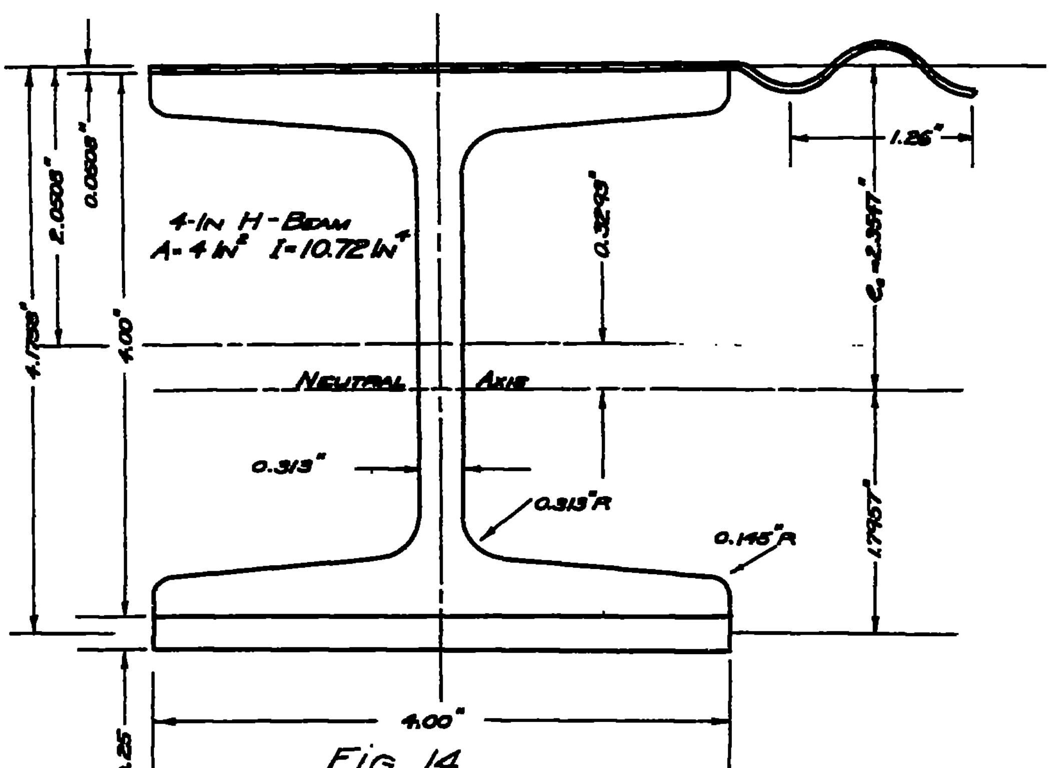

FIG. 14
SIDE BEAM WITH COVER PLATES

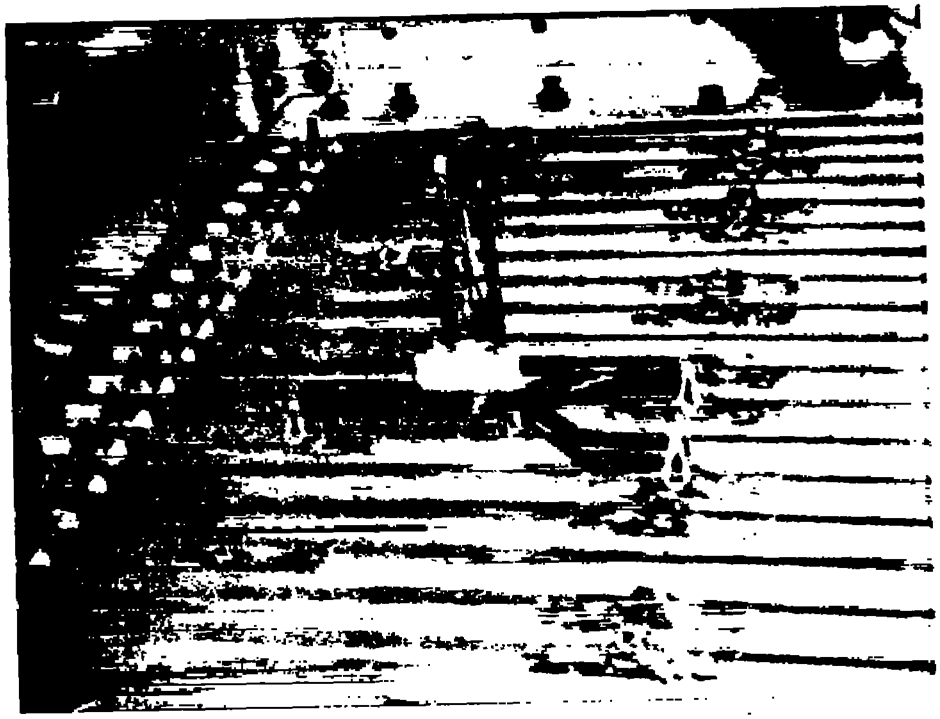

Figure 13.- Detail of Huggenberger tensometer mounting.

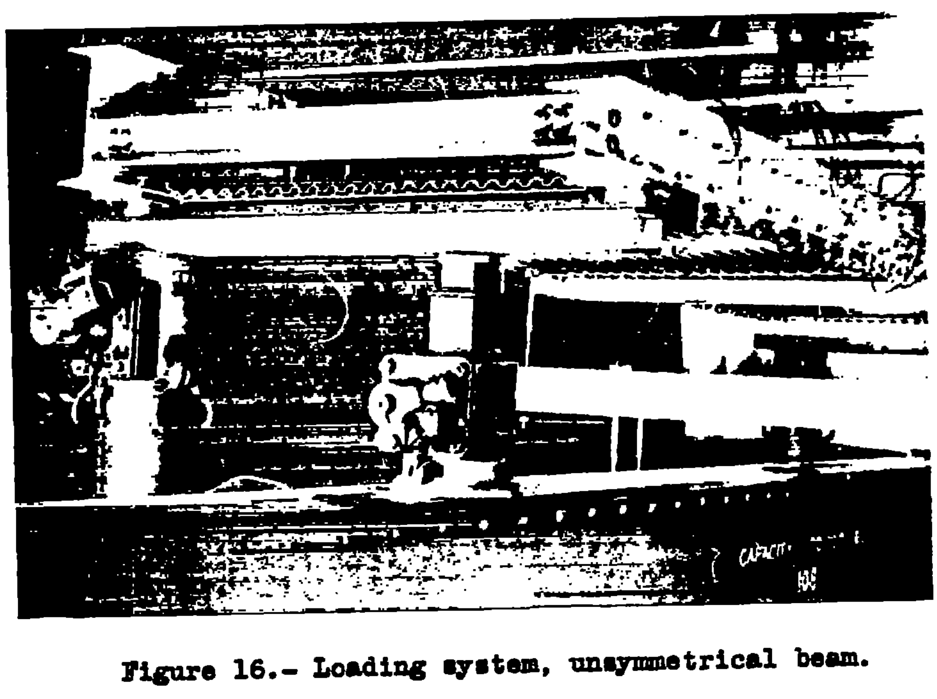

Figure 16.- Loading system, unsymmetrical beam.

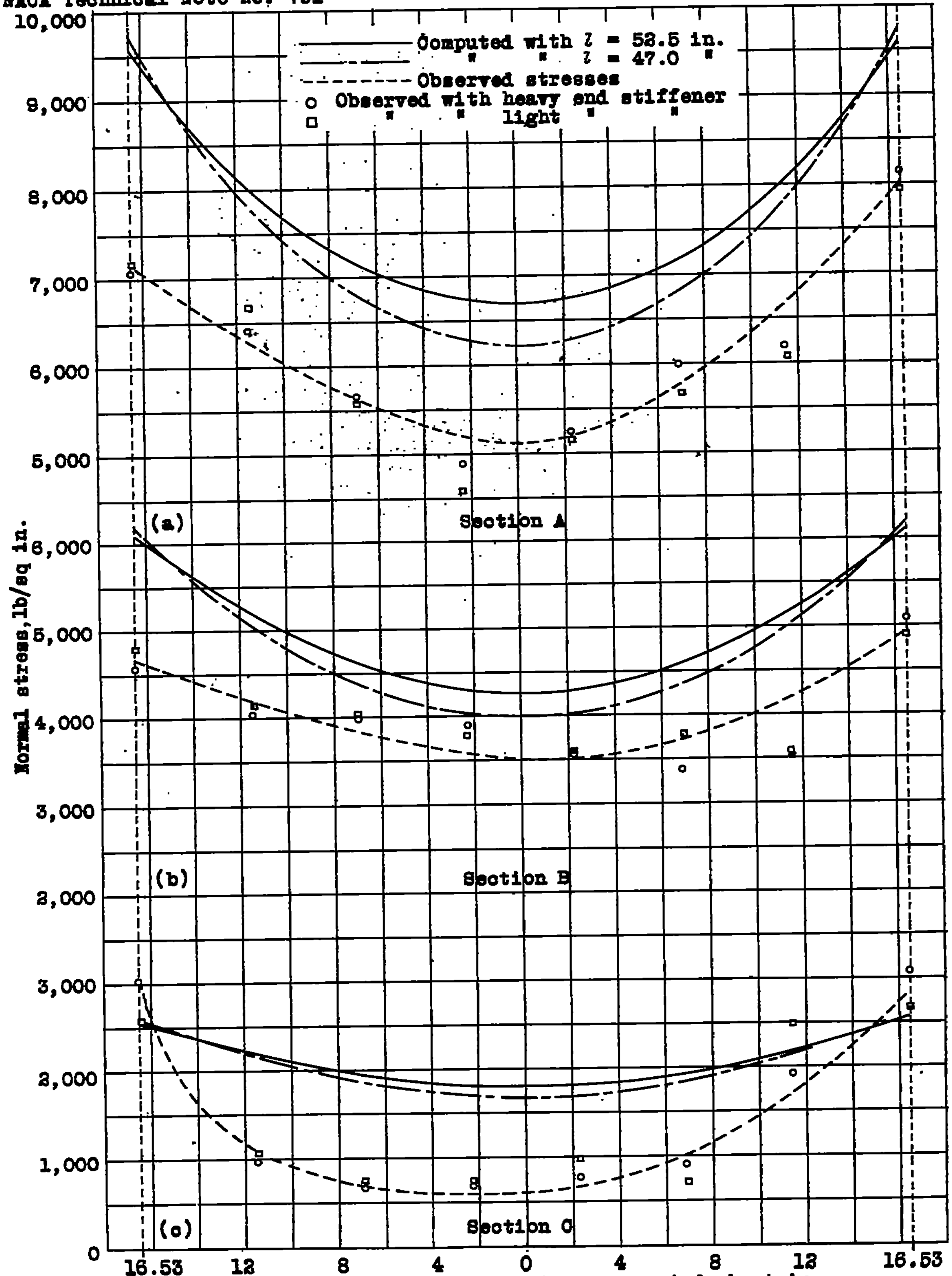

Figure 15.- Comparison of observed and computed stresses.

Figure 17.- Strain gage mounting on unsymmetrical beam.

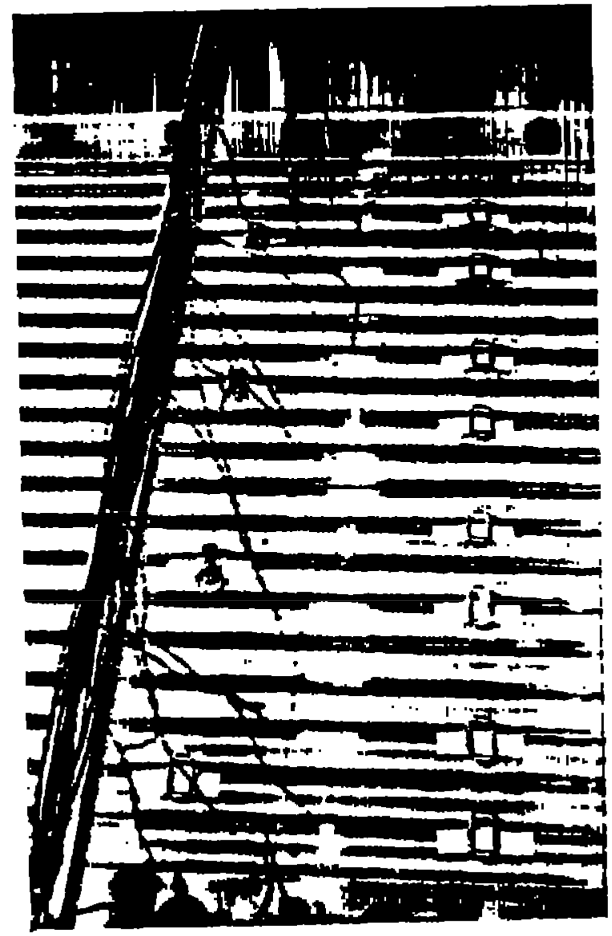

Figure 18.- Transverse view showing strain gages.

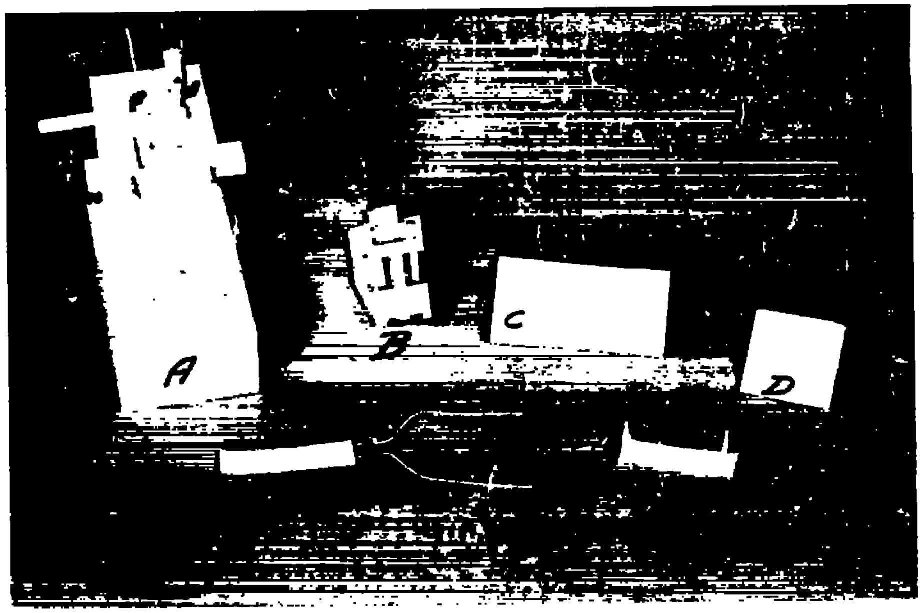

Figure 19a.

Figure 19b.

Figure 19.- Tools for making fine-wire gages.

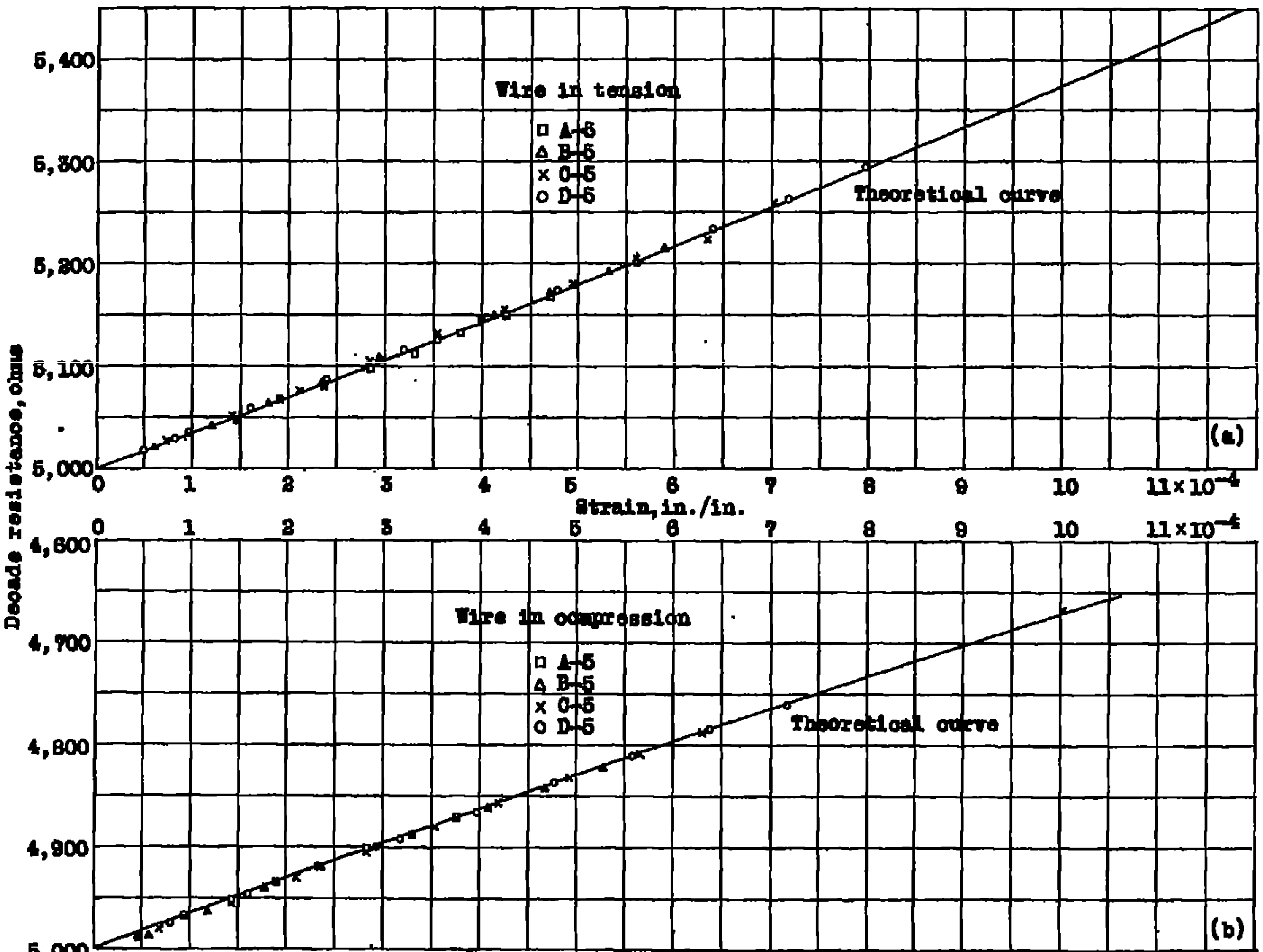

Figure 20.- Calibration chart for wire strain gage.

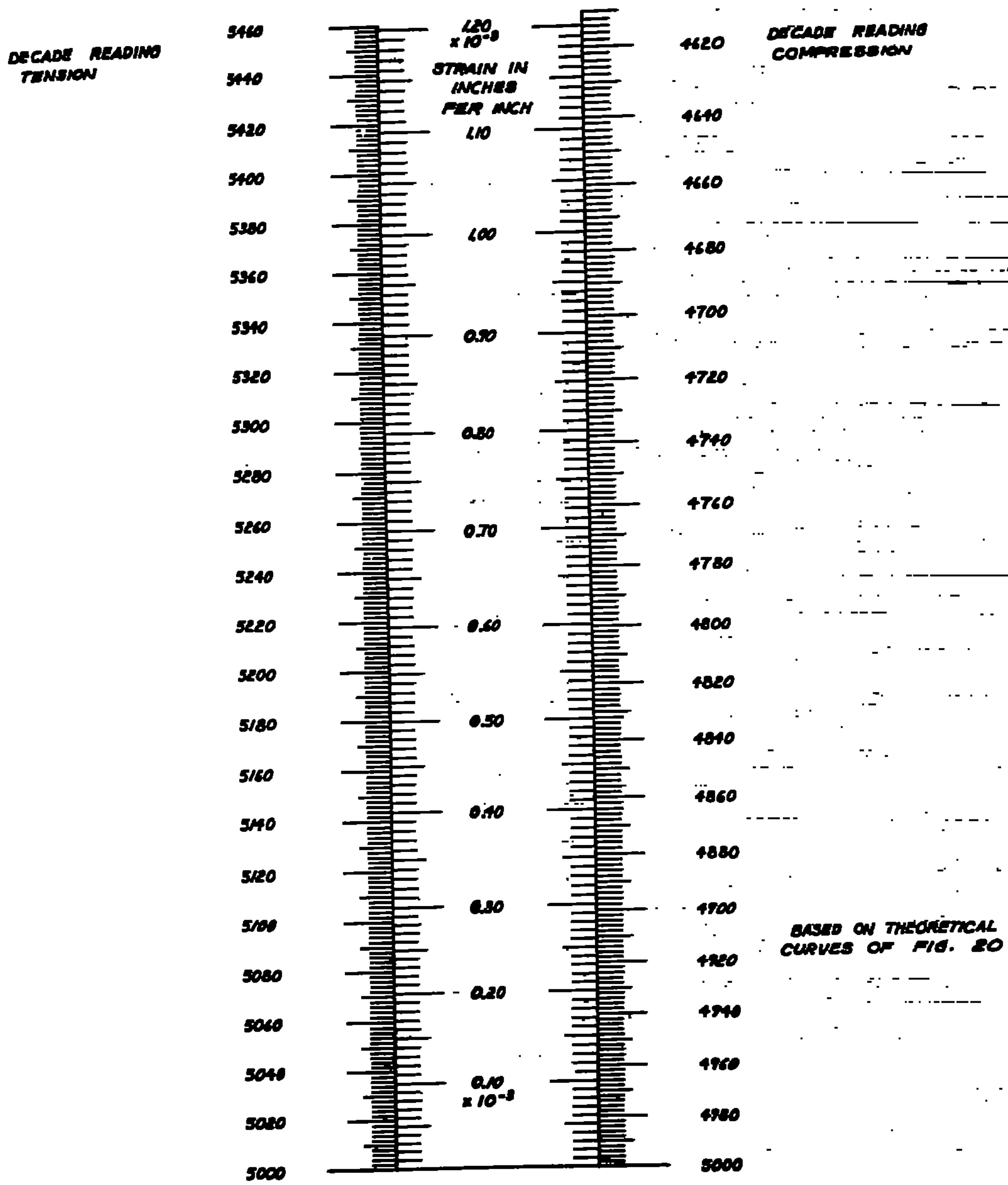

NOMOGRAM FOR STRAIN VS. DECADE READING

FIG. 21

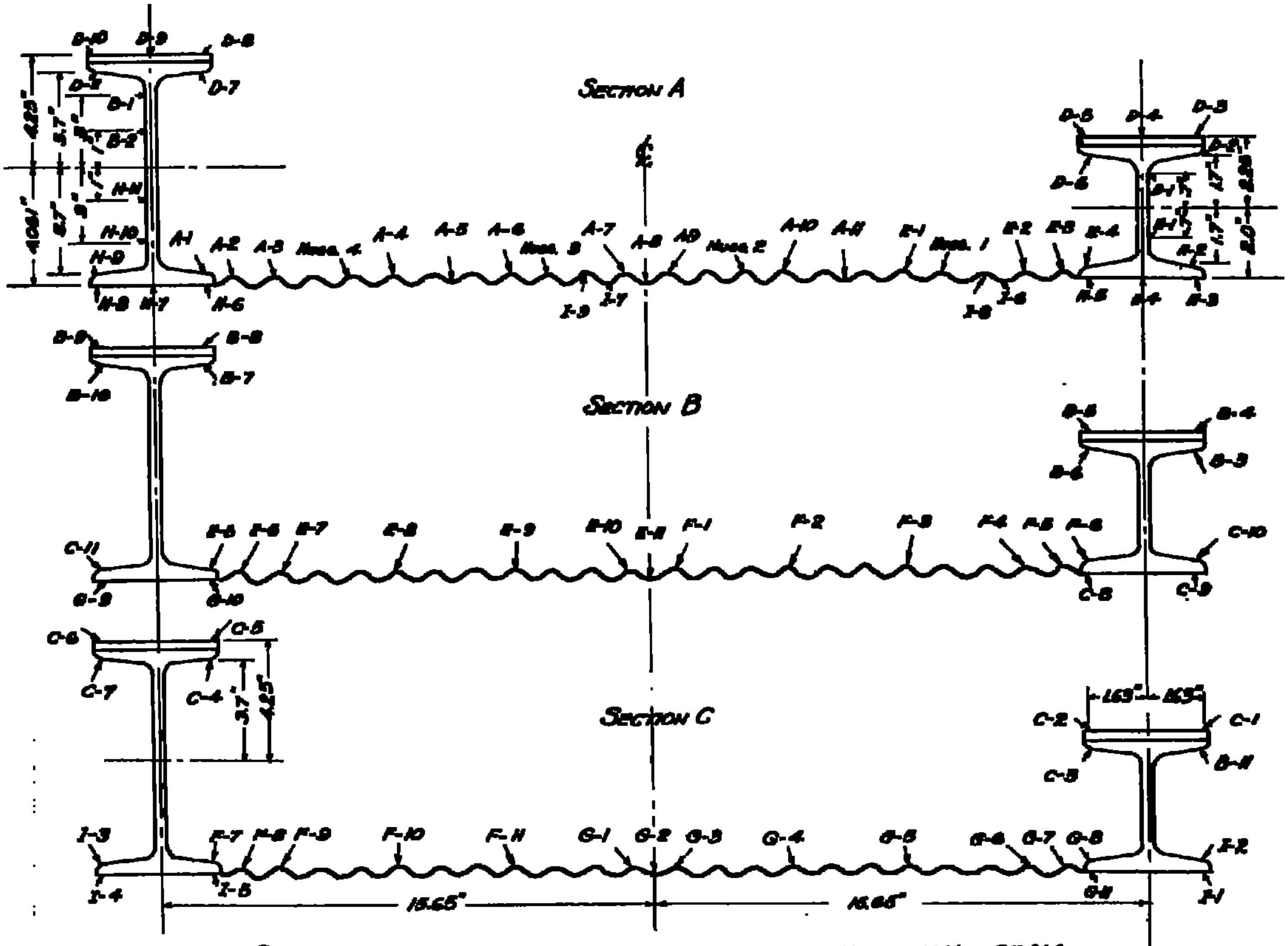

SKETCH SHOWING GAGE POSITIONS FOR THE UNSYMMETRICAL BEAM

FIG. 22

105

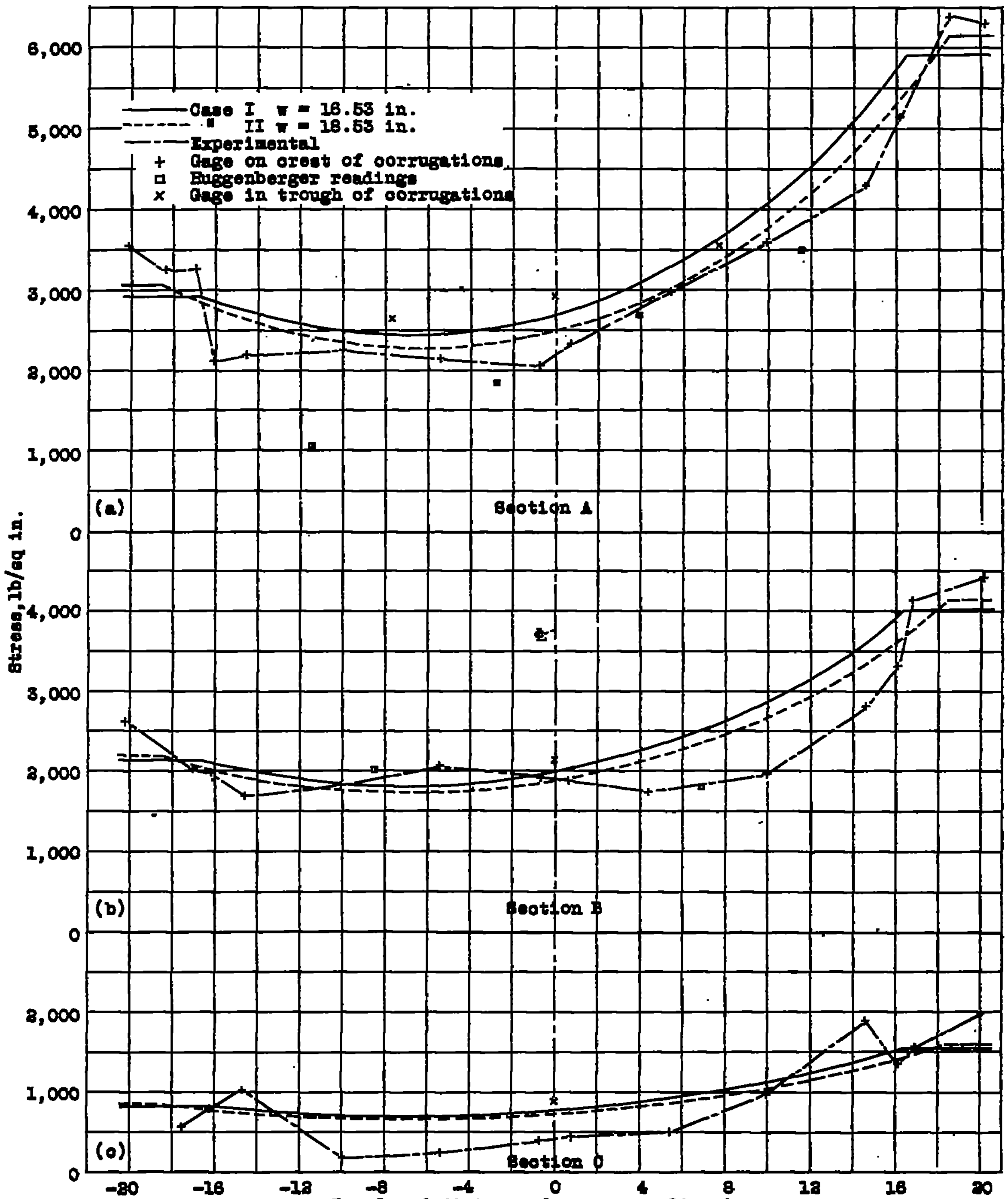

Figure 23.- Stress distribution in the unsymmetrical beam.